Applied GIS

an international, refereed, open source journal

ISSN: 1832-5505

URL: http://www.arts.monash.edu.au/ges/research/Gis/public/epress.html

MANAGING EDITORS:

Jim Peterson - Jim.Peterson@arts.monash.edu.au

Ray Wyatt - ray.wyatt@unimelb.edu.au

Volume 3, Number 1

March, 2007

CONTENTS:

All papers published during 2007 are part of *Volume* 3.
Each paper constitutes one *Number.*

Hence this paper should be cited as:

Ahmad. S. S., and Simonovic. S. P. (2007) – A methodology for Spatial Fuzzy Reliability Analysis, *Applied GIS,* 3(1): 1-42.

Applied GIS Volume 3 (1):1-42

A METHODOLOGY FOR SPATIAL FUZZY RELIABILITY ANALYSIS

Shohan S. Ahmad
Ph.D candidate in Civil and Environmental Engineering Department, The University of Western Ontario, London, Ontario, Canada.
Correspondence to Shohan S. Ahmad: sahmad52@uwo.ca

Slobodan P. Simonovic
Professor in Civil and Environmental Engineering Department, The University of Western Ontario, London, Ontario, Canada.
Correspondence to Slobodan P. Simonovic: simonovic@uwo.ca

Key words: flooding, fuzzy sets, reliability, GIS

Abstract
Natural hazard risk assessment requires quantification of uncertainty that is spatially and temporally variable. Spatial variability of risk has been rarely considered in the past research. This paper presents a new methodology to capture the spatial uncertainty as well as the subjectivity associated with the natural hazard risk analysis. The fuzzy set theory has been integrated with the geographic information system (GIS) in the development of the methodology for spatial reliability analysis. Paper explores the spatial extension of three fuzzy reliability indices i.e. (1) combined reliability-vulnerability, (2) robustness, and (3) resiliency. Fuzzy risk and reliability are quantified within a GIS framework and maps showing spatial variability of three fuzzy indices are developed. The proposed methodology has been applied to flood hazard management. It has been found that the application of spatial fuzzy reliability analysis provides additional information to flood managers regarding the spatial variability of flood risk and aids in the development of a sustainable flood management options.

1. Introduction

Engineering risk and reliability analysis is a general methodology for the quantification of uncertainty and the evaluation of its consequences for the safety of engineering systems (Ganoulis, 1994). Risk identification is the first step in any risk analysis, where all sources of uncertainty are clearly detailed. Quantification of risk is the second step through which uncertainties are measured using different system performance indices and figures of merit such as reliability, vulnerability, robustness and resiliency. Probability theory and fuzzy set theory are the two main approaches used in risk and reliability analysis of engineering systems.

1.1 Probabilistic Reliability Analysis

The probabilistic reliability analysis has been extensively used to deal with the problem of uncertainty in engineering systems (Modarres et al., 1999). The early works of Hashimoto et al. (1982a, 1982b) are the basis for the use of performance indices (i.e. reliability, resiliency, vulnerability, robustness indices) in the evaluation of performance of water resource systems (El-Baroudy and Simonovic, 2004). The probabilistic approach involves describing load and resistance as belonging to respective possible probability distributions. As a result, uncertainty in both, load and resistance is introduced through the use of random variables. The intensive calculations involved in this approach require prior knowledge of the probability density functions of both load and resistance and/or their joint probability distribution functions (El-Baroudy and Simonovic, 2004). The data required to perform such calculations is usually

insufficient and even if data is available to estimate these distributions, approximations are almost always necessary to calculate the system reliability (Ang and Tang, 1984).

There are several approximate methods available to overcome the problem of (a) data insufficiency and (b) inability to address objective and subjective uncertainty in the same time. One approach is the use of subjective judgment of the decision-maker to estimate the probability distribution of a random event, i.e. subjective probability (Vick, 2002). Another approach is the integration of judgment with the observed information using Baye's theory (Ang and Tang, 1984). The problem with Bayesian reliability analysis is in choosing the prior distribution that does not reflect the true uncertainty inherent to the system. The choice of subjective probability distribution, in these two approaches, presents difficulty in translation the prior knowledge into meaningful probability distribution, especially for multi-parameter problems (Press, 2003). Therefore, accuracy of the derived distributions is strongly dependent on the realistic estimation of the decision-maker's judgment (El-Baroudy and Simonovic, 2004).

1.2 Fuzzy Reliability of System Performance

Fuzzy set theory (Zadeh, 1965) was intentionally developed to address people's judgmental beliefs or the uncertainty that results due to lack of knowledge. Relative to the probability theory, it has a certain degree of freedom with respect to aggregation operators, types of fuzzy sets (membership functions), etc., which allows for its adaptability to different contexts (El-Baroudy and Simonovic, 2004). The last twenty years has shown that fuzzy set theory and fuzzy logic have contributed successfully to technological development in different application areas such as mathematics, algorithms, standard models, and real-world problems of different kinds (Zimmermann, 1996). The application of the fuzzy set approach in the field of disaster management has grown over the last two decades. Uncertainty, the lack of knowledge and complexity are expected to be of growing importance in the near future, which support the need to provide trust to the application of the fuzzy set theory (Zimmerman, 1996). The existing fuzzy approaches are used extensively in multi-objective engineering decision making under uncertainty (Kacprzyk and Nurmi, 1998; Bender and Simonovic, 2000; Despic and Simonovic, 2000; Borsuk et al., 2001; Kwok et al., 2002; Prodanovic and Simonovic, 2002; Simonovic and Nirupama, 2005; Akter and Simonovic, 2005; among others). El-Baroudy and Simonovic (2004) developed fuzzy reliability indices: (1) combined reliability-vulnerability, (2) robustness, and (3) resiliency for the evaluation of water resource system performance. The fuzzy reliability indices are able to quantify the reliability, vulnerability, robustness and resiliency of multi-component systems reflecting different systems' configurations in the fuzzy environment.

1.3 Spatial Fuzzy Reliability Analysis

A comprehensive risk and reliability analysis requires generation of appropriate models that consider spatial and temporal characteristics of natural and human induced hazards such as floods, storm surges, cyclones, water and air pollution. Degree of spatial and temporal variability can significantly affect the risk analysis process. GIS can represent risk that is multi-dimensional and spatial in nature (Coppock, 1995). GIS spatial analysis process may contribute to the reduction of uncertainty in natural hazard risk assessment (Rejeski, 1993; Emmi and Horton, 1995; Zerger, 2002). In the earlier research GIS has been used to handle spatial information and assist the decision making process. Foster and McDonald (2000) used GIS for assessment of pollution risks to a surface water intake. Areas of potential hazard to water quality have been identified using GIS based probabilistic modeling. GIS has also been used in probabilistic risk assessment of environmental hazards such as earthquakes, land-slides and accidental spills (Foster and McDonald, 2000). However, application of probabilistic reliability analysis is invariably affected by the well-known engineering problem of data insufficiency and fails to properly address the problem of uncertainty (El-Baroudy and Simonovic, 2004). Makropoulos et

al., (2003) have used fuzzy logic in GIS to handle spatial information and developed a spatial decision support system (SDSS) for urban water management. Simonovic and Nirupama (2005) have developed Spatial Fuzzy Compromise Programming (SFCP) to capture the spatial uncertainty in water resources decision making. SFCP chooses the best alternative for every raster cell from a number of possible alternatives. However, spatial uncertainty associated with natural hazard risk assessment has not yet been addressed.

The applications of fuzzy sets that consider spatial uncertainty is almost non-existent in the literature on natural hazard risk assessment. Most of the existing methods are not capable of spatial representation of risk. Since the natural hazard risk analysis is overwhelmed with spatial variability, a new approach is proposed here (a) to capture the spatial uncertainty in the data, and (b) to spatially represent risk using GIS by extending the concept of fuzzy reliability indices to space. Work presented in this paper deals with extension of the fuzzy reliability analysis to spatial evaluation of uncertainty. In case of floods, droughts, storm surges, cyclones, hurricanes, regional water supply systems, power delivery systems, sewer systems and even environmental pollution, the spatial fuzzy reliability analysis can be used to improve the decision making process.

1.4 Organization of Paper

The following section of the paper describes the theory of fuzzy reliability indices developed by El-Baroudy and Simonovic (2004) and its extension to capture spatial variability in disaster management variables. The next section presents an application case study of the Medway Creek, Ontario, Canada where the spatial fuzzy reliability analysis is used for flood risk assessment. Paper ends with list of conclusions and directions for future research.

2. Spatial Fuzzy Reliability Indices

Engineering reliability analysis uses load and resistance as the fundamental concepts to define the risk of system failure (Simonovic, 1997). System load is defined as the variable that reflects different loading conditions that may be imposed over the useful life of the system (Ang and Tang, 1984). System resistance, on the other hand, is defined as the system characteristic variable which describes the capacity of the system to resist potential loading conditions (El-Baroudy and Simonovic, 2006). These two concepts are widely used in structural engineering to reflect the characteristic behavior of the system under external loading conditions. According to the classical definition, the failure state is the state when resistance falls below the load, margin of safety (i.e., the difference between load and resistance) $M<0.0$ or safety factor (i.e., the ratio between load and resistance) $\Theta<1.0$. However, it is difficult to arrive at a precise definition of failure because of the uncertainty in determining system resistance, load, and the threshold of acceptable unsatisfactory performance. Load and resistance can be represented in fuzzy form to capture the uncertainties involved in their definitions. Fuzzy set theory is then used to calculate the resulting margin of safety (or factor of safety) membership function as a representation of the system state at any time. El-Baroudy and Simonovic (2004) state that it is neither realistic nor practical to have precise identification of failure and that it is more realistic to build in the inevitability of partial failure. As the boundaries of the acceptable failure region are ambiguous and vary from one decision maker to the other depending on the personal perception of risk, these boundaries cannot be determined precisely. Fuzzy sets are capable of representing the notion of imprecision better than the ordinary sets. Therefore, the acceptable level of performance is represented as a fuzzy membership function. For example, in water supply systems the resistance represents supply capacity from different sources, and the actual load represents water demand. Partial failure would describe events when the supply capacity is

insufficient to meet the demand over a short period of time. The boundaries of the partial failure (for example, period without sufficient supply) can be determined by the decision maker.

In flood management for example, resistance can be represented by the elevation of the embankment used to protect an area from flooding and load can be represented by the flood water level. A margin of safety or safety factor can be used as performance functions. Accuracy of flood water levels may vary significantly as well as the elevation of the flood protection embankment. Therefore, the failure state prediction is subject to uncertainty too. Ahmad and Simonovic (2006) have proposed the use of partial failure concept introduced by El-Baroudy and Simonovic (2004) in floodplain management. Partial failure is defined by the introduction of subjective acceptable failure level. Performance of the system in the region between the failure state (in the case of flood management, complete inundation of the protected area) and the acceptable failure level (in case of flood management, partial inundation of the protected area) defines the region of partial failure.

The fuzzy set theory and partial failure concept are used in the development of three fuzzy reliability indices that form the basis of the spatial fuzzy reliability analysis. They are spatial combined fuzzy reliability-vulnerability index; spatial fuzzy robustness index and spatial fuzzy resiliency index. An original methodology is presented in this paper for the computation of fuzzy reliability indices in space using GIS. Computation of the fuzzy reliability indices in space using GIS requires generation of the system state membership function and acceptable level of performance membership function for every grid cell. Spatial risk assessment is performed using commercial GIS software. All the spatial information is analyzed using raster data model. Raster data model contains a number of grid cells defined by rows and columns where the size of the particular pixel defines the cells spatial resolution and each cell contains one piece of information (Makropoulos and Butler, 2004). The following sections describe detailed analytical aspects for calculation of spatial fuzzy reliability indices.

2.1 Fuzzy System State Membership Function in Space

System state membership function can be represented using various shapes as indicated in Figure 1. In this research, a triangular fuzzy membership function is used to represent the fuzzy system state. A system state is defined in GIS by the membership function $\widetilde{S}_i(D)$ on the universe of discourse D, as shown in Figure 2.

$$\widetilde{S}_i(D) = \begin{Bmatrix} 0 & if\ D_i \le D_{i\,Min} \\ \dfrac{D_i - D_{i\,Min}}{D_{Mean} - D_{Min}} & if\ D_i \in [D_{i\,Min}, D_{i\,Mean}] \\ \dfrac{D_{i\,Max} - D_i}{D_{i\,Max} - D_{i\,Mean}} & if\ D_i \in [D_{i\,Mean}, D_{i\,Max} \\ 0 & if\ D_i \ge D_{i\,Max} \end{Bmatrix} \quad (1)$$

where,

$\widetilde{S}_i(D)$ is the system state membership function for the i-th cell;

$D_{i\,Mean}$ is the modal value of the system state; and

$D_{i\,Min}$, $D_{i\,Max}$ are the lower and upper bounds of the system state.

Spatial information of $D_{i\,Min}$, $D_{i\,Mean}$, and $D_{i\,Max}$ are stored in three GIS layers of the same map since the grid cell in a raster image can contain only a single spatial information.

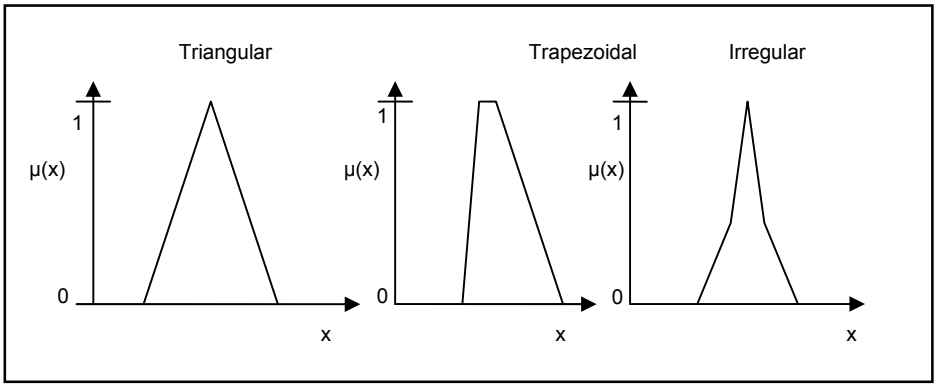


Figure 1 Different shapes of fuzzy system state membership function

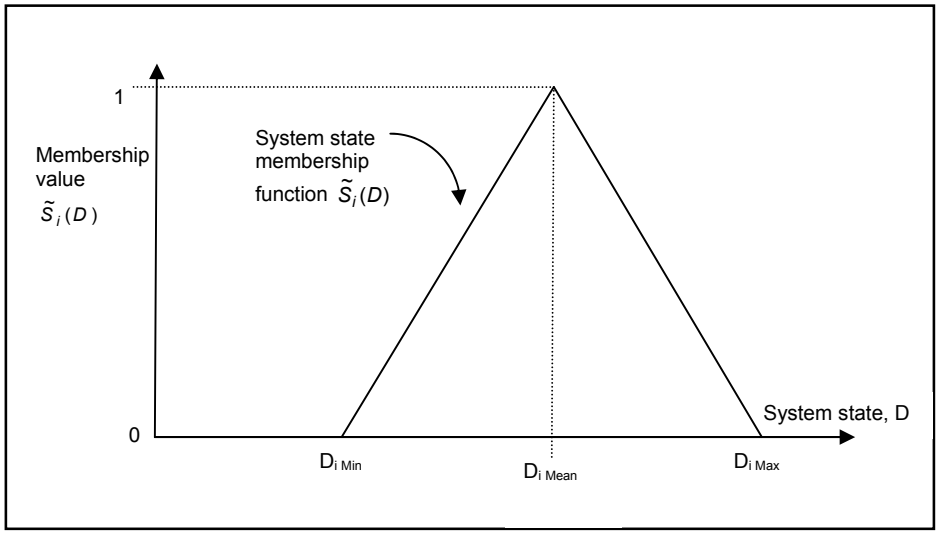


Figure 2 System state membership function

2.2 Fuzzy Acceptable Level of Performance in Space

Fuzzy acceptable level of performance is set for every cell in the raster image. The acceptable level of performance is represented as a fuzzy membership function, $\tilde{M}_i(D)$, based on the system state value D.

$$\tilde{M}_i(D) = \begin{Bmatrix} 1 & if\ D_i \le D_{i1} \\ \theta(D_i) & if\ D_i \in [D_{i1}, D_{i2}] \\ 0 & if\ D_i \ge D_{i2} \end{Bmatrix} \quad (2)$$

where,
$\widetilde{M}_i(D)$ is the fuzzy membership function of margin of safety for cell i; and
D_{i1} and D_{i2} are lower and upper bounds of acceptable level of performance.

If the system state value is above D_{i2}, then the system performance is completely unacceptable (Figure 3). In this case the membership function $\widetilde{M}_i(D)$ has zero value. If the system state value is below D_{i2} but above D_{i1}, then the system performance is partially acceptable. The membership function, $\widetilde{M}_i(D)$ of the acceptable level of performance attains its peak (unity) if the system state value is less than D_{i1}. The system performance at this stage is considered completely safe.

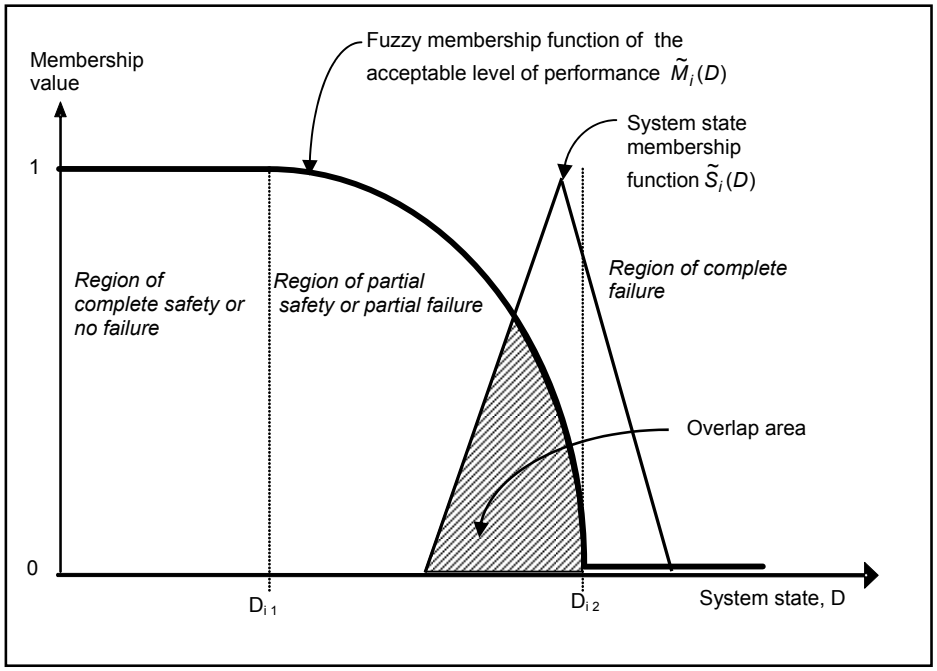


Figure 3 Fuzzy representation of the acceptable level of performance

2.3 Fuzzy Reliability and Fuzzy Compatibility

Reliability Measure (LR_i) of the acceptable level of performance is calculated for every grid cell in the raster image as follows:

$$LR_i = \frac{D_{i1} \times D_{i2}}{D_{i2} - D_{i1}} \tag{3}$$

For a particular acceptable level of performance the value of D_{i1} and D_{i2} are constant for every grid cell in the raster image. Therefore, the value of reliability measure (LR_i) is same in a map for a single acceptable level of performance.

Fuzzy compatibility (CM_i) between the system state membership function and the fuzzy acceptable level of performance membership function is the basis for the calculation of the combined fuzzy reliability-vulnerability index. It is expressed as follows:

$$CM_i = \frac{Weighted\ overlap\ area}{Weighted\ area\ of\ the\ system\ state\ function} \quad (4)$$

Weighted area of the system state membership function and the weighted overlap area between the acceptable level of performance membership function and the system state membership function are calculated in GIS for determining the measure of compliance (Figure 3).

First, the system state membership function (Figure 4) computed for each cell is subdivided into a number of layers and the weighted area of a single segment of the system state membership function is calculated in GIS using,

$$dA_{i\,w} = \left[\frac{(D_{i\,rl} - D_{i\,11}) + (D_{i\,r2} - D_{i\,12})}{2}\, ds\right]\left[\widetilde{S}_{i\,\alpha}(D) + \frac{ds}{2}\right] \quad (5)$$

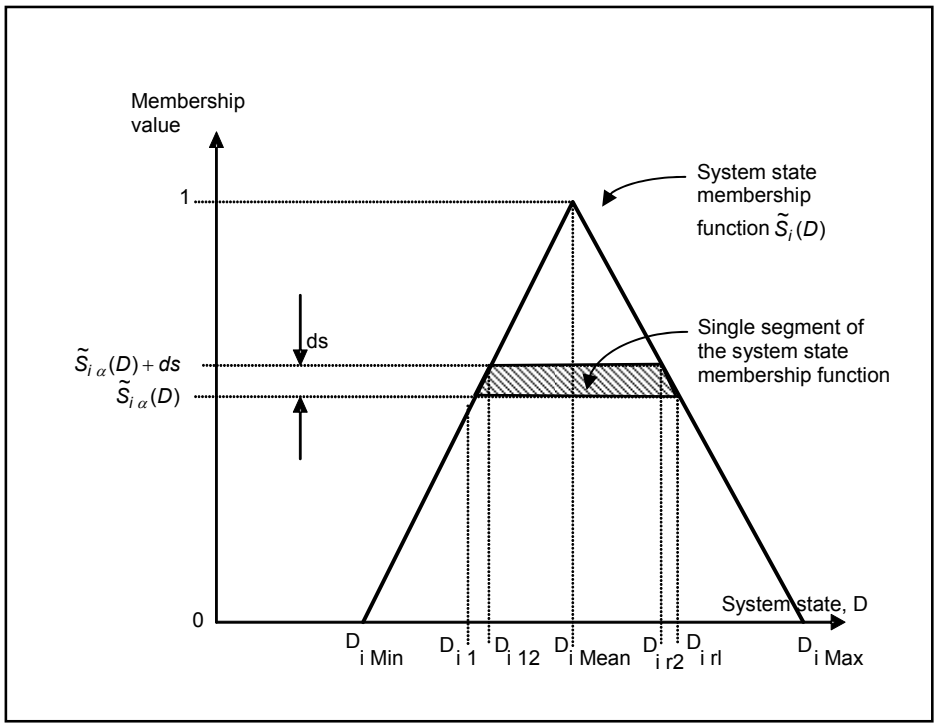


Figure 4 Weighted area calculation for the system state membership function

Similarly the weighted area for each segment of the system state membership function is calculated using Equation (5) and summed up to give the total weighted area of the system state membership function. As a result the raster image containing cells with high value of system state have a larger membership function area than cells with medium value of system state and low value of system state (Figure 5). This also affects the weighted area of the system state membership function.

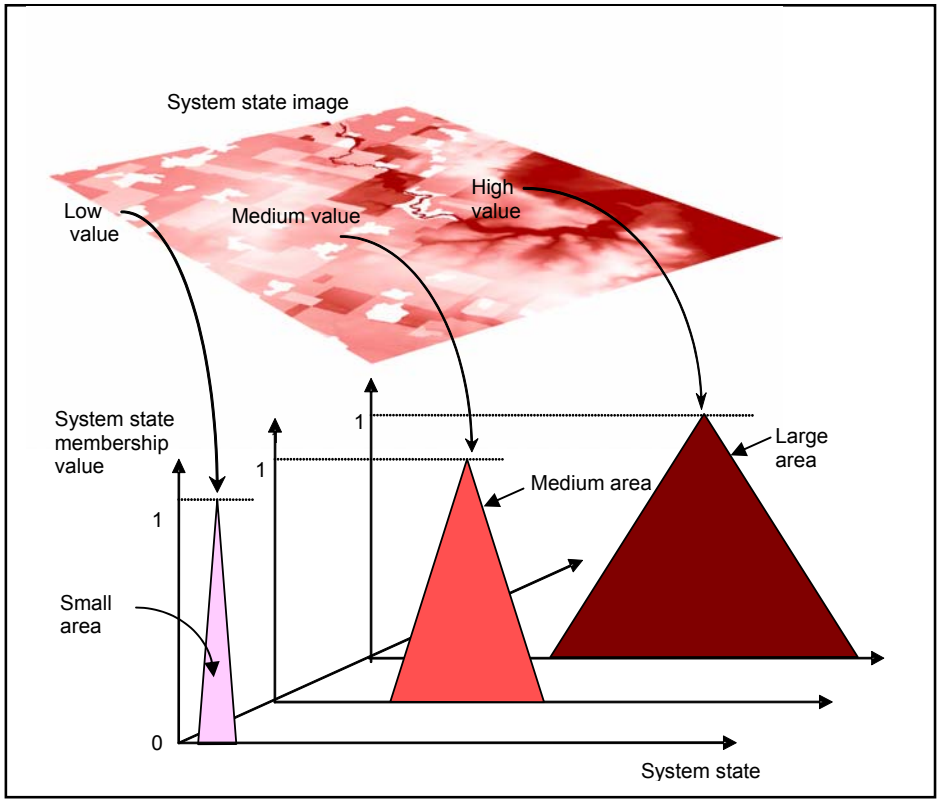


Figure 5 Triangular membership functions for different values of the system state

The weighted overlap area between the acceptable level of performance membership function and the system state membership function are calculated in GIS by considering four possible scenarios (Figure 6):

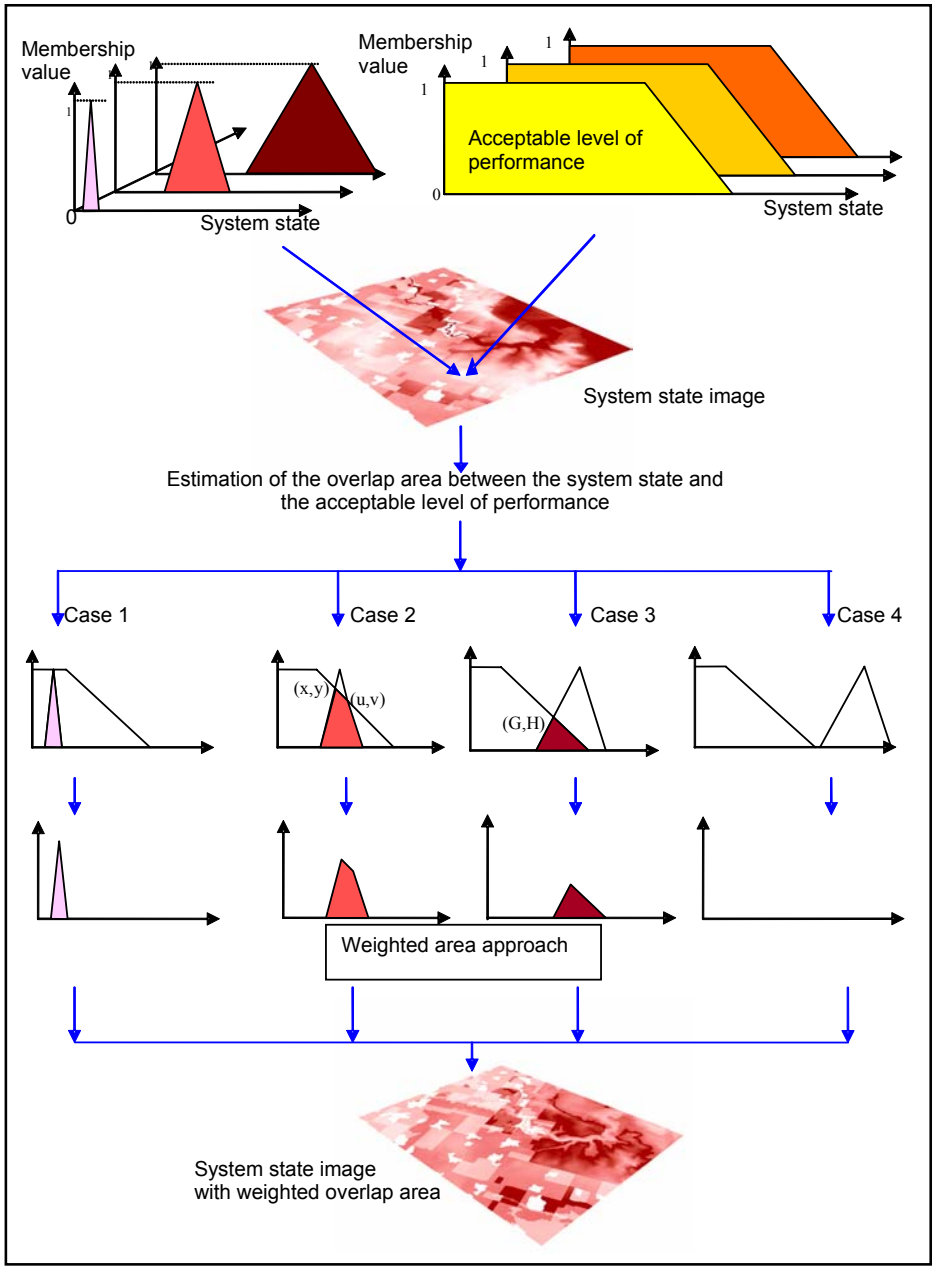


Figure 6 Flow chart for generation of weighted overlap area between the system state and acceptable level performance in GIS

Case 1 - Complete overlap of the acceptable level of performance membership function and system state membership function. So, the weighted overlap area has the same value as the weighted system state in GIS;

Case 2 - Partial overlap of the acceptable level of performance membership function and the system state membership function. This overlap area is determined in GIS by locating the intersection points i.e. (x,y) and (u,v) (Figure 6). Then the weighted overlap area is calculated using Equation (5);

Case 3 - This case represents less compliance compared to the second case. The weighted overlap area is calculated by locating one intersection point i.e. (G,H) between the acceptable level of performance membership function and the system state membership function and then using the weighted area approach; and

Case 4 - No overlap between the acceptable level of performance membership function and the system state membership function (Figure 6). This case results in zero compliance and fuzzy compatibility is assigned a zero value.

Overlay operation and spatial analyst tool in GIS, are used in all four cases to determine the weighted overlap area from a number of raster images. Layers containing the system state will have different value for each cell. Another layer that contains a predefined acceptable level of performance has the same value for every grid cell containing the same feature. For example, the decision maker can set the different acceptable level of performance for land, roads and buildings or use the same for all the features. The output of the compatibility analysis is a single raster map representing the compliance of the system state with a predefined acceptable level of performance in the raster image.

2.4 Spatial Combined Fuzzy Reliability-Vulnerability Index

Fuzzy reliability and fuzzy compatibility of two input membership functions are used in mathematical derivation of the combined fuzzy reliability-vulnerability index. *"Reliability and vulnerability are used to provide a complete description of system performance in case of failure and to determine the magnitude of the failure event"* (El- Baroudy and Simonovic, 2004). Spatial combined fuzzy reliability-vulnerability index is calculated for each grid cell in GIS:

$$RE_i = \frac{\max\limits_{f \in K}\left\{CM_{i1}, CM_{i2}, ...CM_{if}\right\} \times LR_{i\max}}{\max\limits_{f \in K}\left\{LR_1, LR_2 .....LR_f\right\}} \quad (6)$$

where:
RE_i is the spatial combined fuzzy reliability-vulnerability index for the i-th cell;
$LR_{i\max}$ is the reliability measure of the acceptable level of performance corresponding to the system state with maximum compatibility value for the i-th cell;
LR_f the reliability measure of the f-th acceptable level of performance;
CM_{if} is the compatibility measure for system state with the f-th acceptable level of performance for the i-th cell;
K is the total number of the defined acceptable levels of performance;
i is the subscript of grid cells, and i=1,2,3,4,…….N; and
N is the total number of grid cells.

The maximum fuzzy compatibility resulting form the consideration of different acceptable levels of performance (i.e. conservative, neutral and risky) (Figure 7), is used together with the reliability measure of acceptable level of performance corresponding to the system state with maximum compatibility value and the maximum of the reliability measure in the Equation 6.

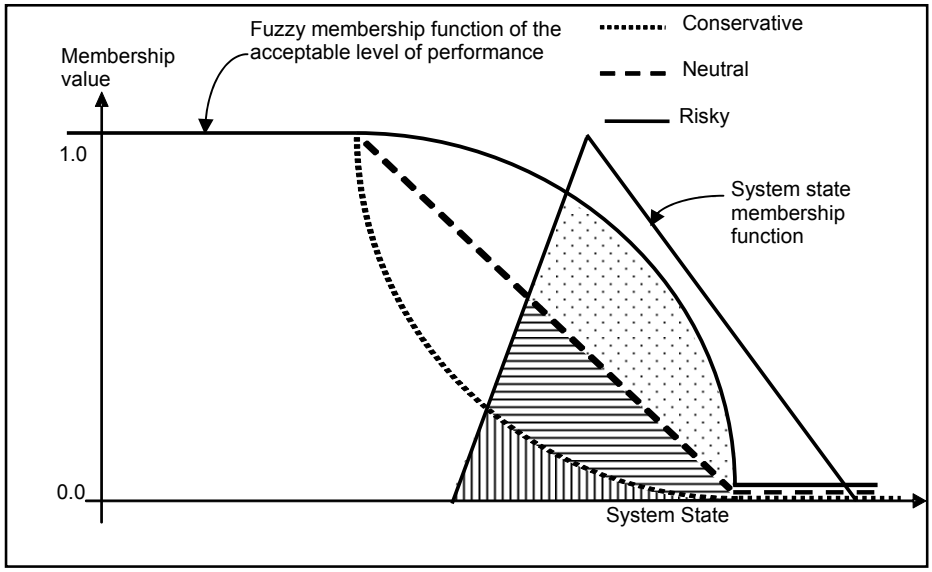


Figure 7 Various shapes of the acceptable level of performance membership function

A flow chart in Figure 8 shows the process adopted for the calculation of the spatial combined fuzzy flood reliability-vulnerability index. Computation of combined fuzzy reliability-vulnerability index in GIS comprises of six steps. In the first step triangular fuzzy membership functions are used to describe the uncertainty in flood damage. Spatial information of lower bound, modal value and upper bound of flood damage are stored in three GIS layer. In the second step, weighted area of the flood damage membership function is spatially analyzed in GIS using Equation (5) which resulted in a single raster map. In the third step three acceptable levels of flood damage i.e. (i) conservative level (first acceptable level of flood damage), (ii) neutral level (second acceptable level of flood damage), and (iii) risky level (third acceptable level of flood damage) for buildings and lands are assigned for every grid cell in the raster map. The forth step deals with the computation of weighted overlap area for three acceptable levels of damage. Then in step five, fuzzy compatibility is calculated using Equation (4). Three acceptable levels of damage resulted in three raster maps containing values of fuzzy compatibility. In the last step, Equation (6) is used to develop a single map containing spatial combined fuzzy reliability-vulnerability index.

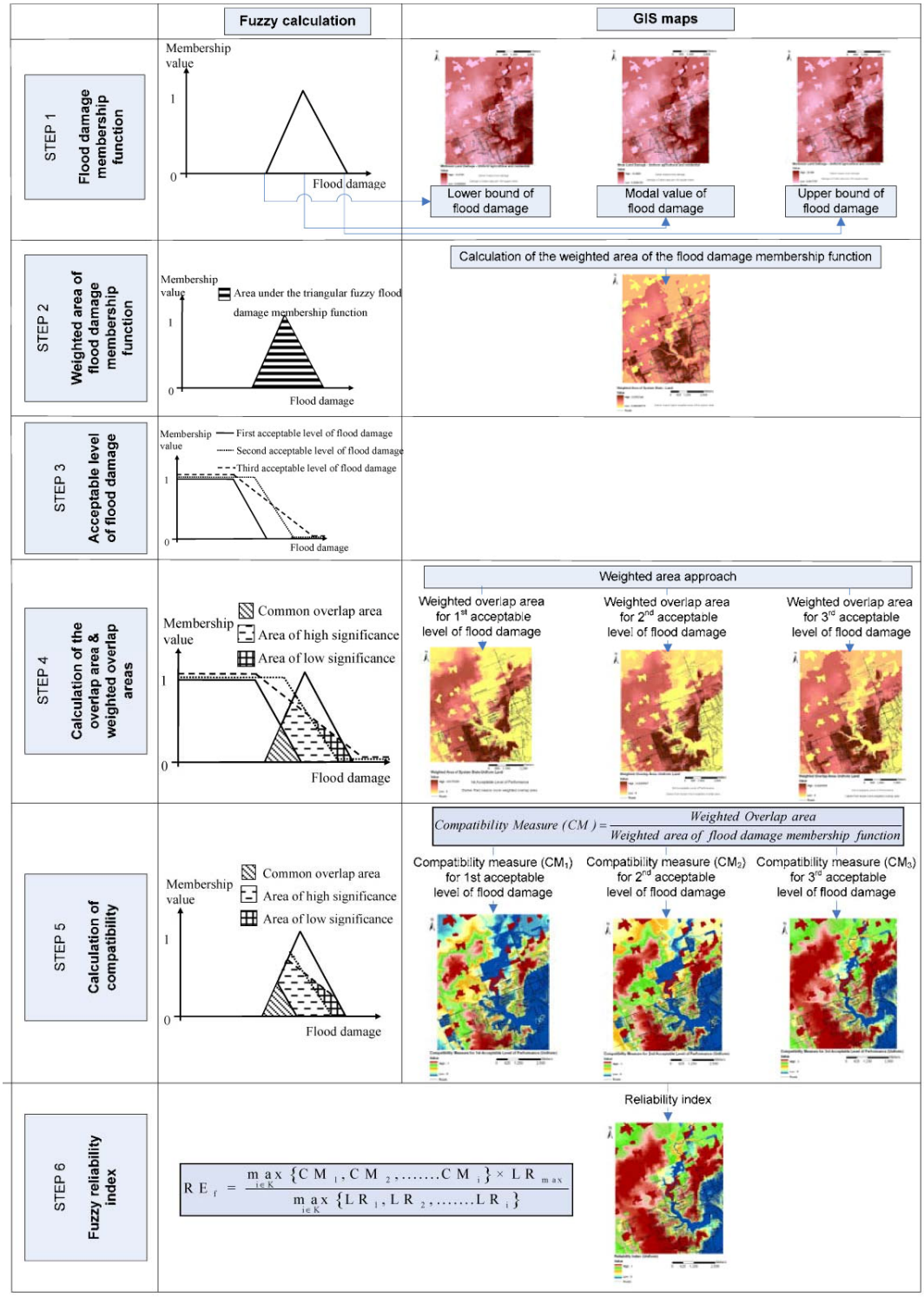


Figure 8 Flow chart for the calculation of the spatial combined fuzzy flood reliability-vulnerability index

2.5 Spatial Fuzzy Robustness Index

The adaptability of the system to change in the acceptable level of performance is spatially represented in GIS. Two maps containing compatibility values for two levels of performance are used as inputs in the following equation:

$$RO_i = \frac{1}{CM_{i1} - CM_{i2}} \quad (7)$$

where:

RO_i is the spatial fuzzy robustness index for the i-th cell;

CM_{i1} is the compatibility value before the change in the acceptable level of performance for the i-th cell;

CM_{i2} is the compatibility value after the change in acceptable level of performance for the i-th cell;
i is the subscript of grid cells, and i=1,2,3,4,…….....N; and
N is the total number of grid cells.

The inverse of the difference in compatibility values between the two acceptable levels of performance is calculated in each cell of the GIS using spatial analyst tool to give the spatial fuzzy robustness index. The spatial fuzzy robustness index is developed for three cases (Figure 7): change of the acceptable level of performance from: (i) conservative to neutral; (ii) neutral to risky; and (iii) conservative to risky.

The calculation process of spatial fuzzy robustness index is performed in six steps, as illustrated in Figure 9. Calculation process of the fuzzy robustness index is the same in the first five steps as for the spatial combined fuzzy reliability-vulnerability index. Robustness index represents the ability of a system to adopt when the acceptable level of performance (or damage) is changed from one level to another. For the illustration of methodology two acceptable levels of flood damage are shown in Figure 9. As a result two maps of spatial fuzzy compatibility are obtained from two acceptable levels of flood damage. In the sixth step Equation (7) is used to obtain a single map of the spatial fuzzy robustness index.

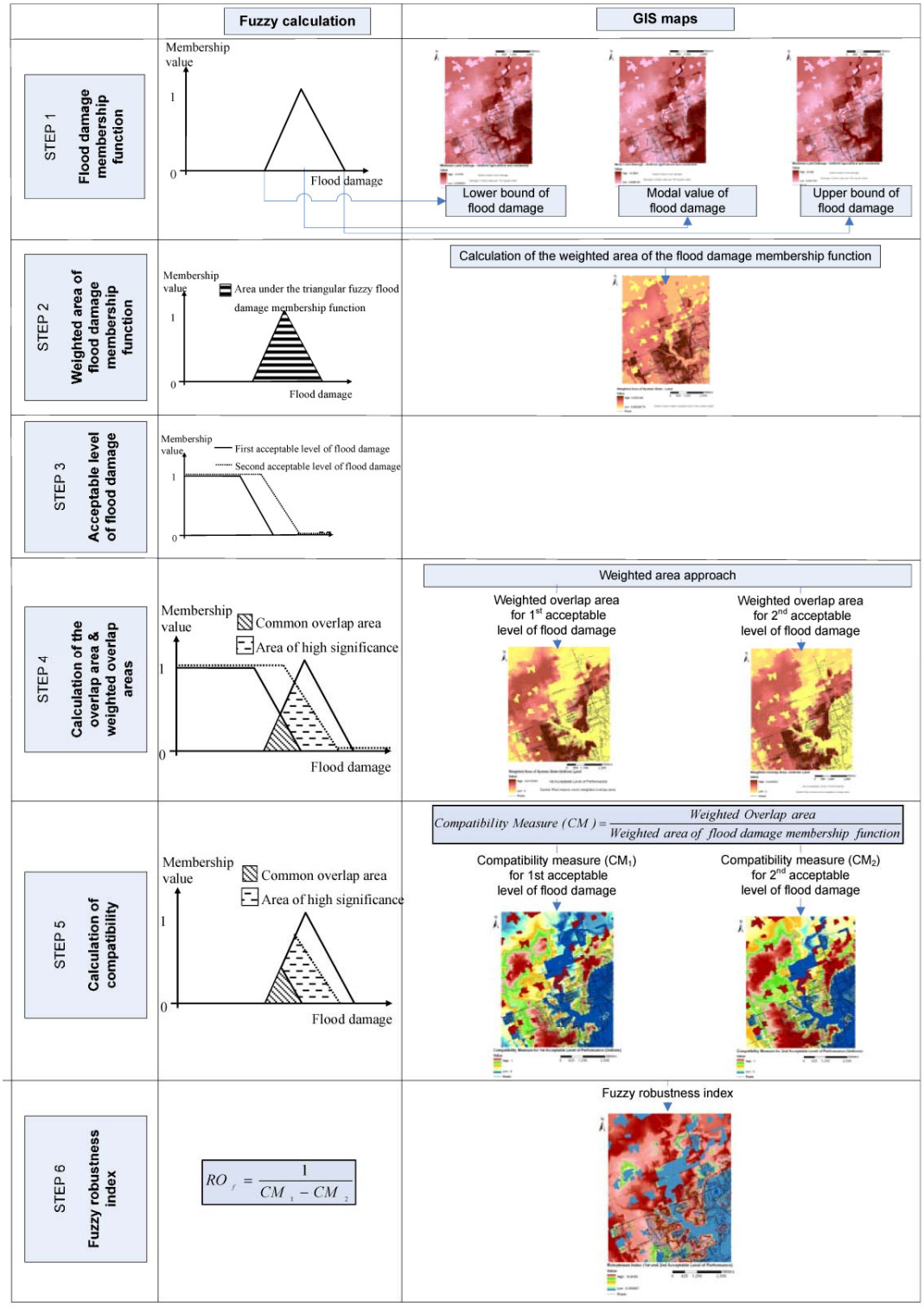


Figure 9 Flow chart for the calculation of the spatial fuzzy flood robustness index

2.6 Spatial Fuzzy Resiliency Index

Resiliency index measures the ability of system to recover from the failure state. Uncertainty in the value of recovery time is captured using a triangular membership function (Figure 10) to convey the notion that the minimum and maximum recovery time values ($t_{i\,1}$ and $t_{i\,3}$) are concentrated around the modal value of the recovery time $t_{i\,2}$ and expressed mathematically as follows:

$$\widetilde{S}_i(t) = \begin{Bmatrix} 0 & if\ t_i \le t_{i1} \\ \dfrac{t_i - t_{i1}}{t_{i2} - t_{i1}} & if\ t_i \in [t_{i1}, t_{i2}] \\ \dfrac{t_{i3} - t_i}{t_{i3} - t_{i2}} & if\ t_i \in [t_{i2}, t_{i3}] \\ 0 & if\ t_i \ge t_{i3} \end{Bmatrix} \quad (8)$$

where,
$\widetilde{S}_i(t)$ is the membership function of the recovery time for the i-th cell;
$t_{i\,2}$ is the modal value of the recovery time for the i-th cell; and
$t_{i\,1}$, $t_{i\,3}$ are the lower and upper bounds of the recovery time for the i-th cell.

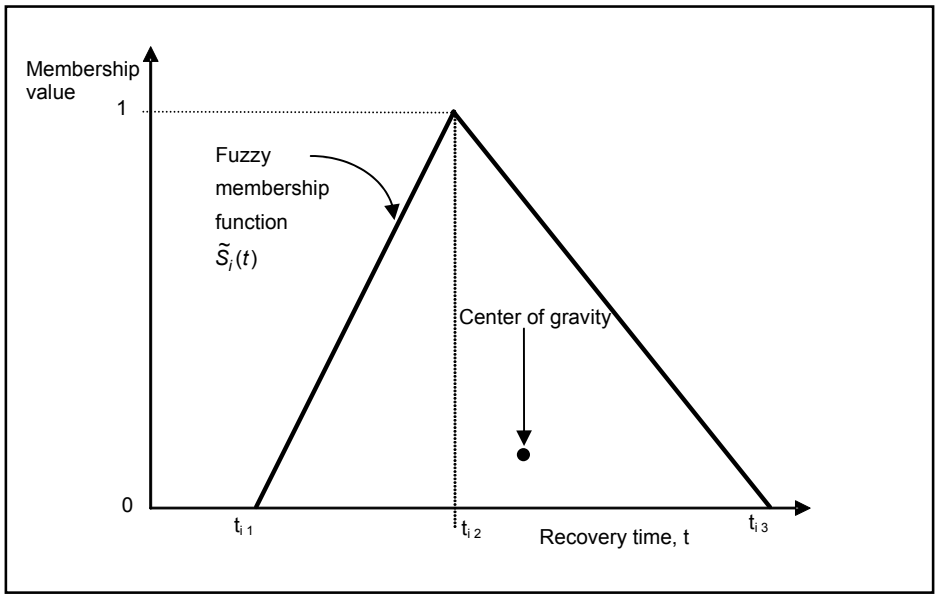


Figure 10 Fuzzy membership function of the recovery time

The maximum of the fuzzy recovery time is used to represent the recovery time. The inverse of the center of gravity of the recovery time is used to spatially represent the resiliency in a single map. Based on the El-Baroudy and Simonovic (2004) definition of resiliency index the computation within GIS is done according to:

$$RS_i = \left[CG_i\right]^{-1} = \left[\frac{\int_{t_{i1}}^{t_{i3}} t_i \widetilde{T}_i(t)dt}{\int_{t_{i1}}^{t_{i3}} \widetilde{T}_i(t)dt}\right]^{-1} \quad (9)$$

where,
RS_i is the spatial fuzzy resiliency index for the i-th cell.
CG_i is the center of gravity of the recovery time membership of the i-th cell;
i is the subscript of grid cells, and i=1,2,3,4,…….....N;
N is the total number of grid cells; and
$\widetilde{T}_i(t)$ is the fuzzy recovery time for the i-th cell.

Three GIS layers are used to store the spatial information on recovery time i.e. t_1, t_2 and t_3 Equation 9 is spatially implemented in GIS to result in resiliency index for every grid cell in a single raster data model.

A flow-chart in Figure 11 shows a detailed process used for spatial calculation of fuzzy flood resiliency index. Step one deals with development of a floodplain map. In step two, the flood water level is varied by a certain range to capture the uncertainty associated with data that results in three maps containing values of water depth (i.e. minimum, modal and maximum flood water). From the stage-damage relationship, flood damage is calculated in step three for land and buildings in the floodplain region. Recovery time is calculated from the damage-recovery time relationship. A triangular fuzzy membership function is generated in step five to account for the uncertainty with respect to recovery time. In this step the maximum recovery time resulting from a number of failure events is selected to identify the highest risk. In step six, Equation (9) is used to calculate the spatial fuzzy resiliency index.

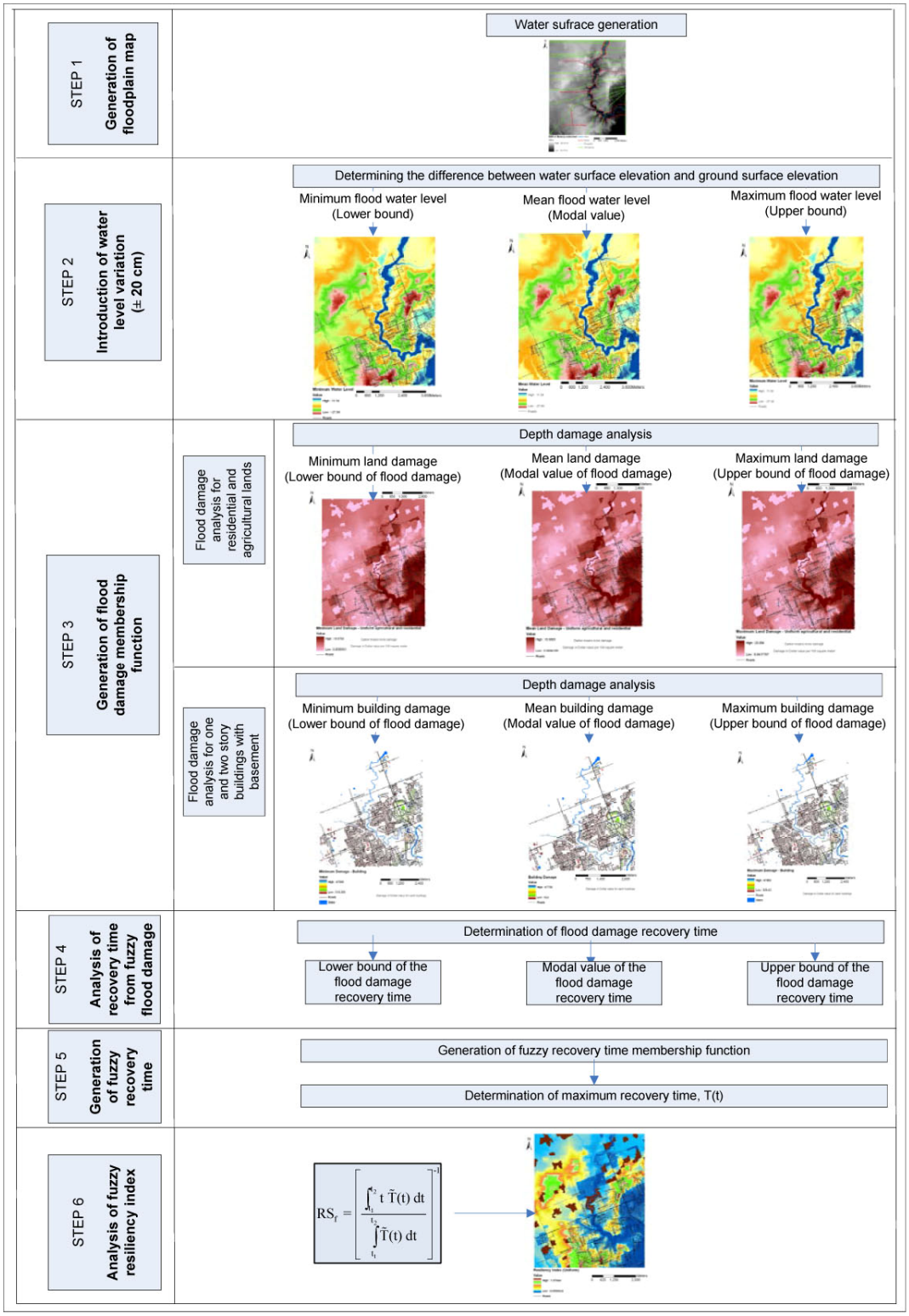


Figure 11 Flow chart for the calculation of the spatial fuzzy flood resiliency index

3. Application of the Spatial Fuzzy Reliability Analysis to Flood Management

The concept of three spatial fuzzy reliability indices: (1) combined reliability-vulnerability, (2) robustness, and (3) resiliency have been tested in the context of fuzzy flood reliability analysis (Ahmad and Simonovic, 2006). The Medway Creek, within the City of London, Ontario, Canada (Figure 12) is chosen as a study area to illustrate the floodplain analysis, and to assess developed spatial fuzzy reliability indices. Flood reliability analysis of the Medway Creek is carried out from Arva to the confluence of Medway Creek and the North Thames River (the area marked by the red box in Figure 12). Inflow data, water level information, hydraulic properties, ground surface elevation, land use data, spatial location of objects (i.e. buildings, roads, water bodies), and relationship between flood water depth and damage are all subject to uncertainty in the flood risk analysis. The fuzzy system state is expressed as fuzzy flood water depth, fuzzy flood damage and fuzzy recovery time and the acceptable level of performance is expressed as acceptable level of flood damage.

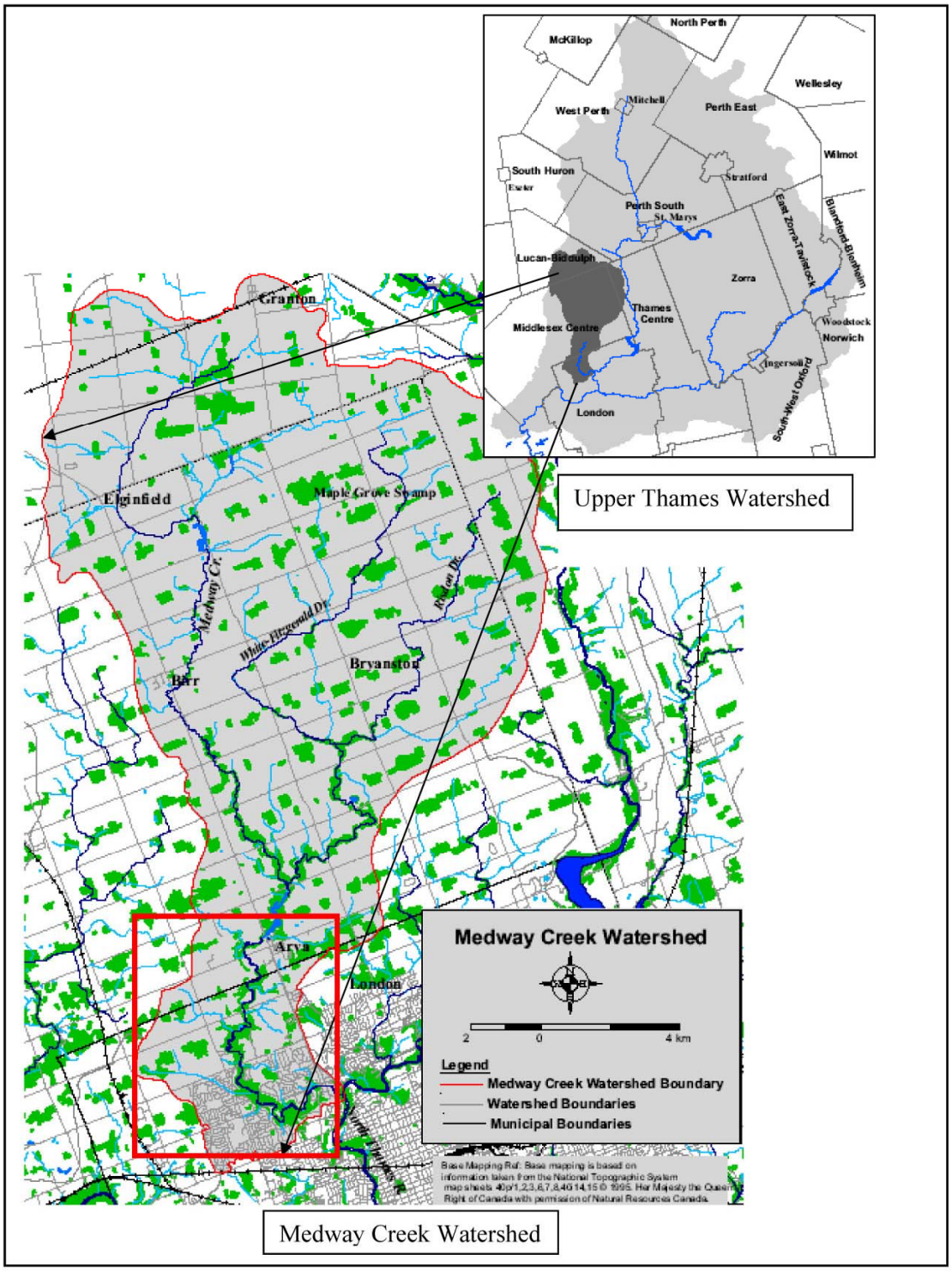


Figure 12 Medway Creek Watershed (Source: UTRCA report card, 2001)

3.1 Data

Digital Elevation Model (DEM) with respect to the UTM projected coordinate system for zone 17N is used for the Medway watershed (Figure 13). A feature image containing the type of land use (Figure 14), ortho-imagery (Figure 15) and polygon features (Figure 16) of the City of London containing shape files of roads as well as building structures are also used. The hydraulic data for the Medway Creek is used in flood plain simulation. The hydraulic data (Figure 17) include flow values for 2 year, 5 year, 10 year, 25 year, 50 year, 100 year and 500 year return periods at specific cross-sections of the Medway Creek. The stage-damage curve for flood damage assessment in the Medway Creek floodplain is developed based on the available data from “Flood Damage Estimation Guide - Ontario Ministry of Natural Resources (Ontario Ministry of Natural Resources, 1990).

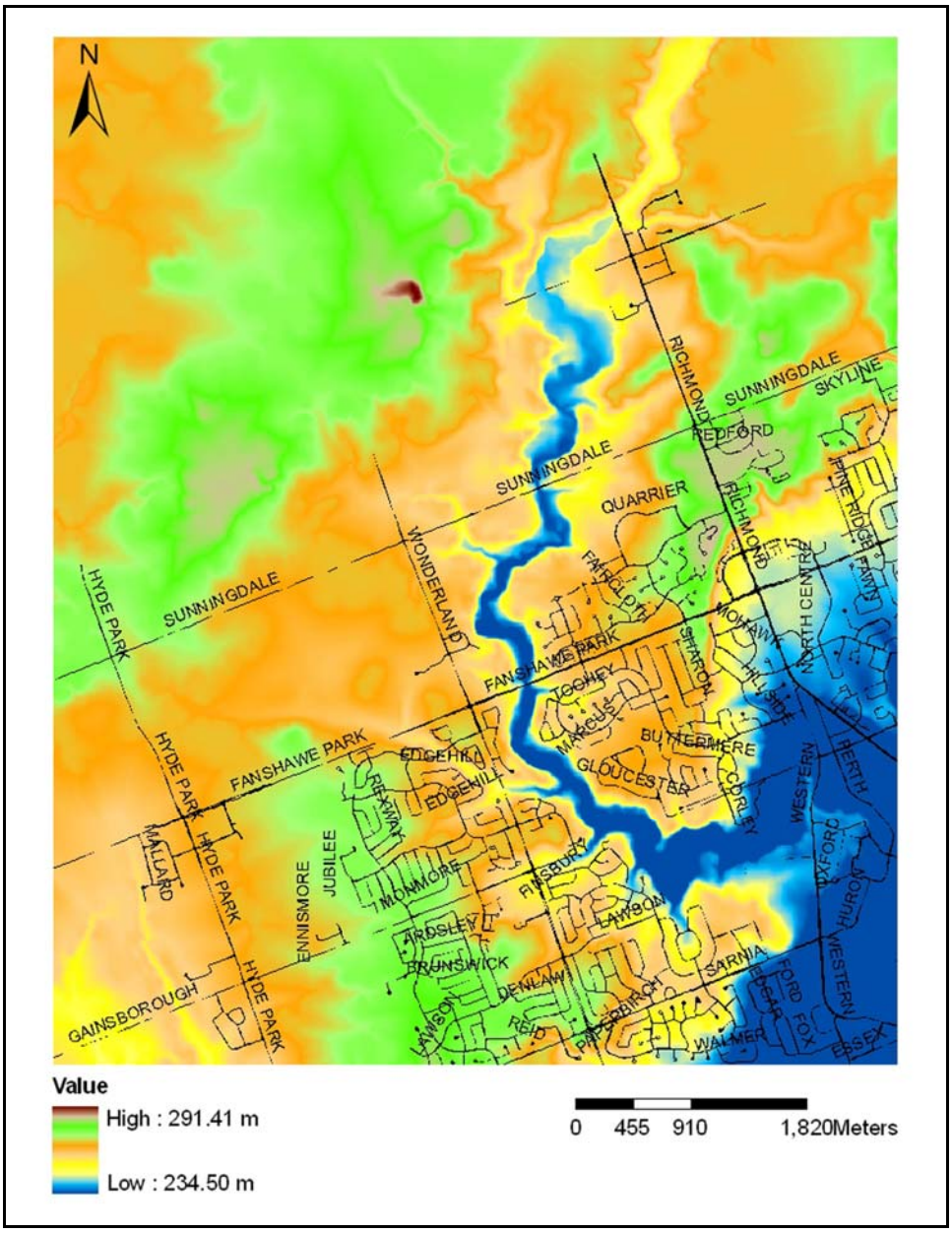


Figure 13 DEM of the Medway watershed

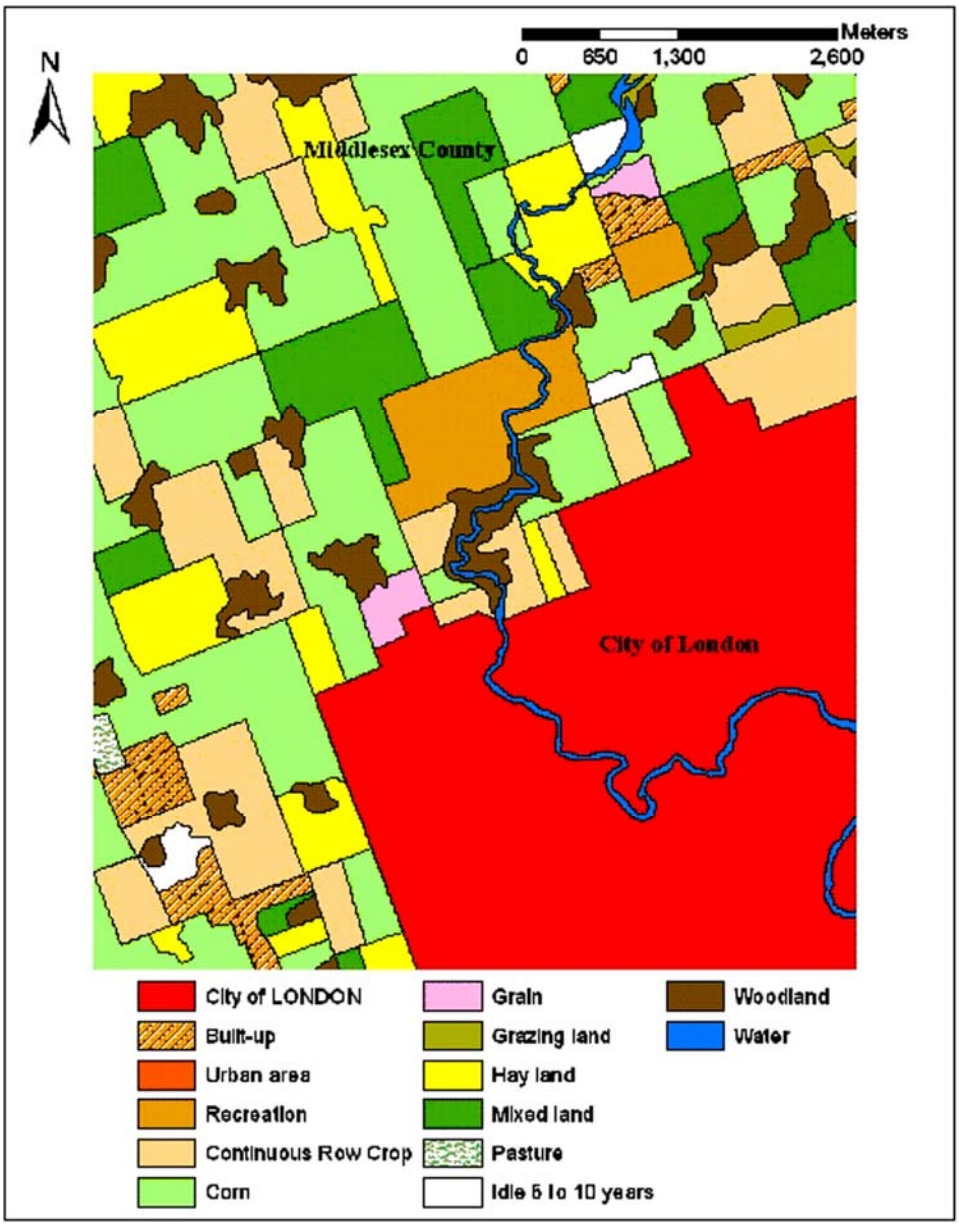


Figure 14 Land-use classification (1983) of the study area in Medway watershed

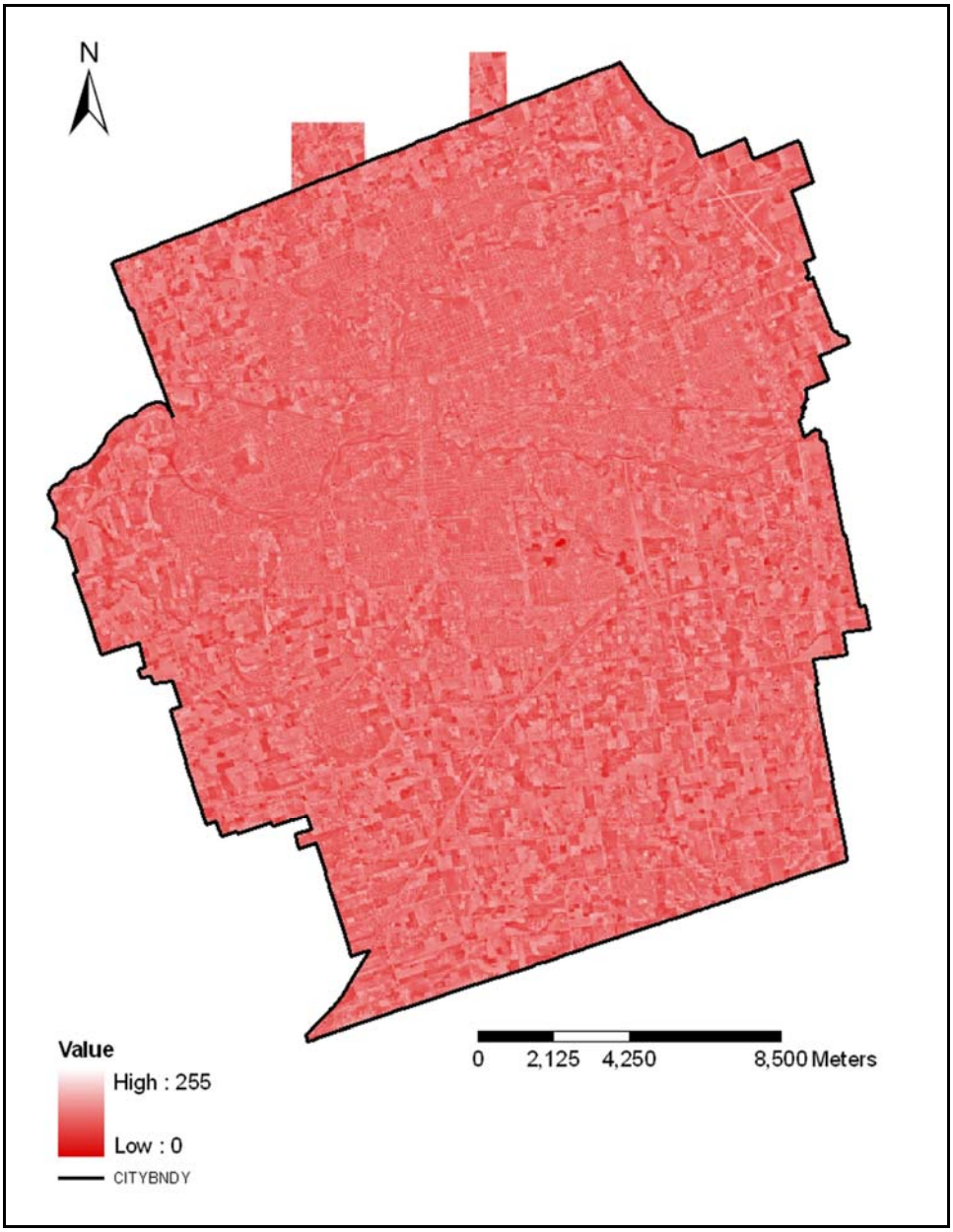


Figure 15 Ortho-photo (2004) of the City of London

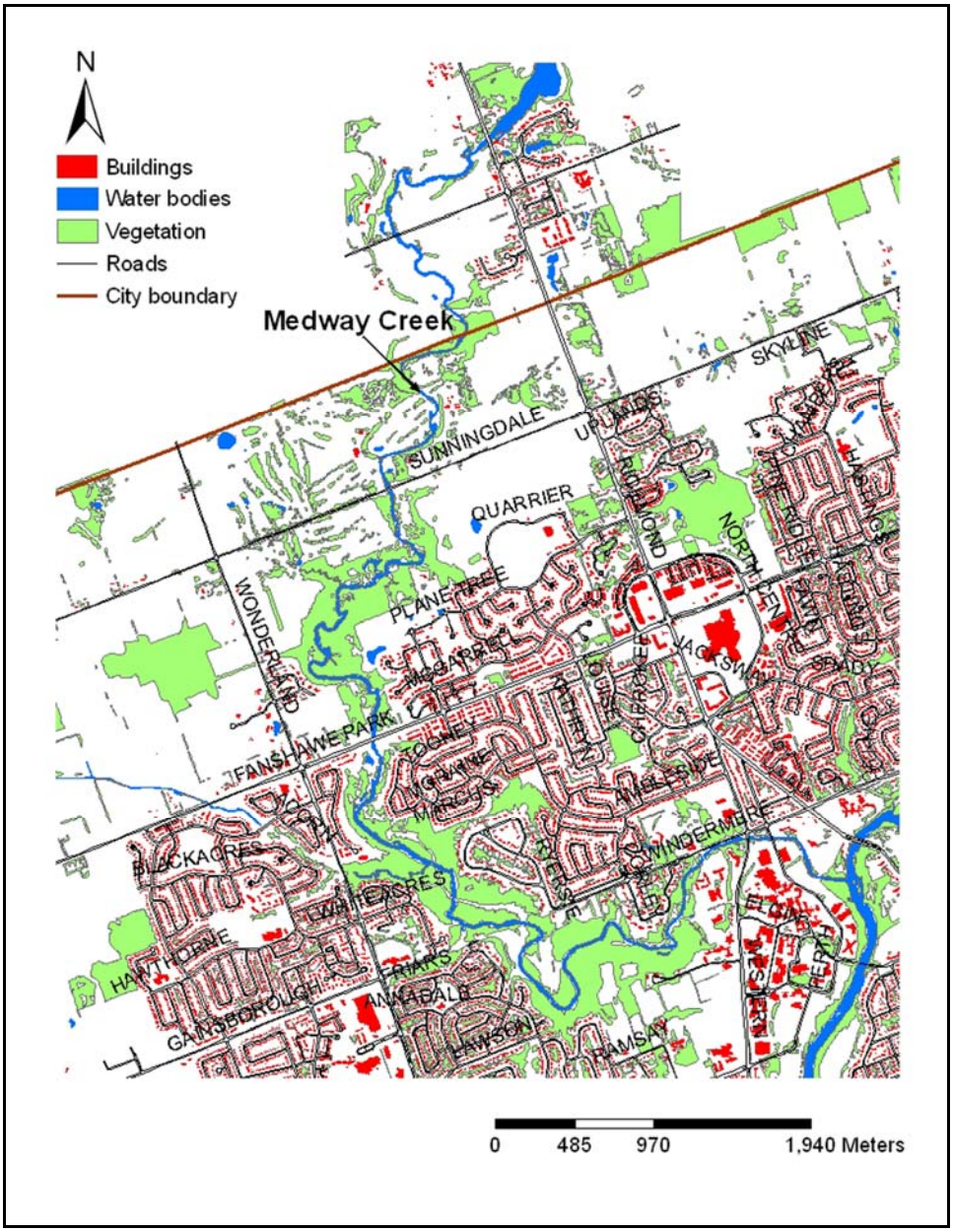
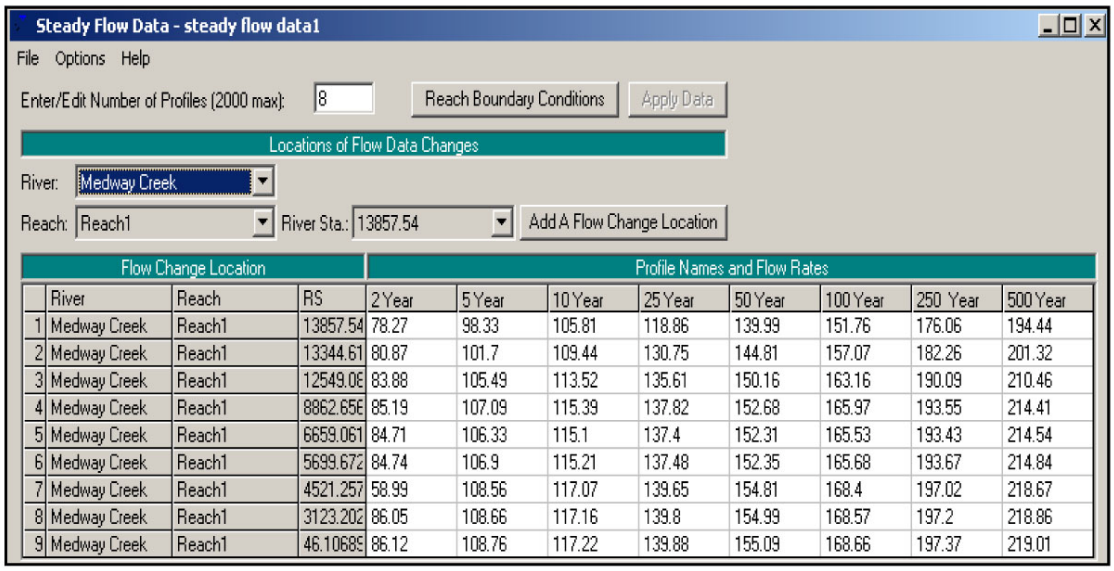


Figure 16 Polygon features of buildings, water bodies and roads in the Medway watershed



Steady Flow Data - steady flow data1

File Options Help

Enter/Edit Number of Profiles (2000 max): 8 Reach Boundary Conditions Apply Data

Locations of Flow Data Changes

River: Medway Creek

Reach: Reach1 River Sta.: 13857.54 Add A Flow Change Location

	Flow Change Location			Profile Names and Flow Rates							
	River	Reach	RS	2 Year	5 Year	10 Year	25 Year	50 Year	100 Year	250 Year	500 Year
1	Medway Creek	Reach1	13857.54	78.27	98.33	105.81	118.86	139.99	151.76	176.06	194.44
2	Medway Creek	Reach1	13344.61	80.87	101.7	109.44	130.75	144.81	157.07	182.26	201.32
3	Medway Creek	Reach1	12549.08	83.88	105.49	113.52	135.61	150.16	163.16	190.09	210.46
4	Medway Creek	Reach1	8862.656	85.19	107.09	115.39	137.82	152.68	165.97	193.55	214.41
5	Medway Creek	Reach1	6659.061	84.71	106.33	115.1	137.4	152.31	165.53	193.43	214.54
6	Medway Creek	Reach1	5699.672	84.74	106.9	115.21	137.48	152.35	165.68	193.67	214.84
7	Medway Creek	Reach1	4521.257	58.99	108.56	117.07	139.65	154.81	168.4	197.02	218.67
8	Medway Creek	Reach1	3123.202	86.05	108.66	117.16	139.8	154.99	168.57	197.2	218.86
9	Medway Creek	Reach1	46.10685	86.12	108.76	117.22	139.88	155.09	168.66	197.37	219.01

Figure 17 Hydraulic flow data used in HEC-RAS for nine river stations

3.2 Medway Creek Floodplain Mapping and Damage Assessment

HEC-GeoRAS (a spatial extension of ArcGIS software) is used in this research for importing the geometric data of the digital terrain from GIS into the hydraulic model (HEC-RAS) for hydraulic calculations (HEC, 2005). River names/IDs; reach names/IDs; cross-sectional cutlines; flowpath lines; stream centerline attributes; bank stations; and downstream reach length for left overbank, main channel and right overbank are created in the HEC-GeoRAS (Figure 18) and all these geometric information are exported to HEC-RAS by creating a RASGIS import file (Figure 19). After the hydraulic computations using the 500 year flow in HEC-RAS, water surface results are imported back into GIS for spatial floodplain delineation. Flood water depth is calculated by subtracting ground surface elevation, available in the DEM, from the calculated water surface elevation and this floodplain map is made clearer by interpolating the resulting floodplain map with a new reclassification of 12 water level zones (Figure 20). As a result the flood water depth in the flood affected areas of the DEM is shown with positive value of water depth. The difference in elevation between the ground surface and the water surface is also analyzed for the regions that are not affected by flooding; therefore shown with negative value of water depth. The maximum flood water depth is shown in dark blue that ranges from 1.8 to 3.5 m. Regions near the Medway Creek and the confluence show high flood water depth. Regions in the map shown in light blue range from (-2.82 to 0.82 m) of flood water depth and result in basement flooding. The range of (-27.5m to -19.05m) shown in dark red represents higher ground elevation compared to the range of (-15m to – 13.2m) shown in green. The floodplain map is converted into the three flood plain maps containing maximum, modal (Figure 20) and minimum flood water levels by introducing ± 20 cm variation in water level to account for uncertainty in the hydraulic analysis. Land and building damage maps (Figure 21 and Figure 22) are produced considering floodplain maps containing flood water level. Flood damage assessment is carried out using depth-damage relationship for one and two story buildings, residential, and agricultural land. Since the resolution of the DEM is ten meters, damage value is assigned for 100 m^2 in every grid cell of the map. It is seen that the residential damage for the built-up area, recreational area and towns are higher (shown in dark red ranging from $8 to $20 per 100 m^2) than the agricultural damage (shown in lighter red ranging from $0.5 to $7.9 per 100 m^2) as damage increases as land closer to the river is being utilized (Figure 21). It is also

observed that the agricultural damage varies with type of crop harvested. For example, land growing grain corn experiences higher damage ($6 to $10) than land growing hay ($2.8 to $4.5). The damage to wooded area is minimal ($0 to $0.4) and is shown in light red on the map in Figure 21. Building damage is illustrated using a color ramp where blue means high damage, yellow and orange means moderate damage, and green and brown means low damage (Figure 22). The red box in the building damage map is zoomed in and the damage values are reclassified in 8 ranges (Figure 23) that show the variation of building damage more clearly. It is observed that few buildings in the study region are built in the high flood risk zones. However, buildings near the confluence of the Medway Creek and the North Thames River are expected to experience significant damage from flooding event and the extent of building damage increases to a maximum of $47000 as buildings get closer to the river front.

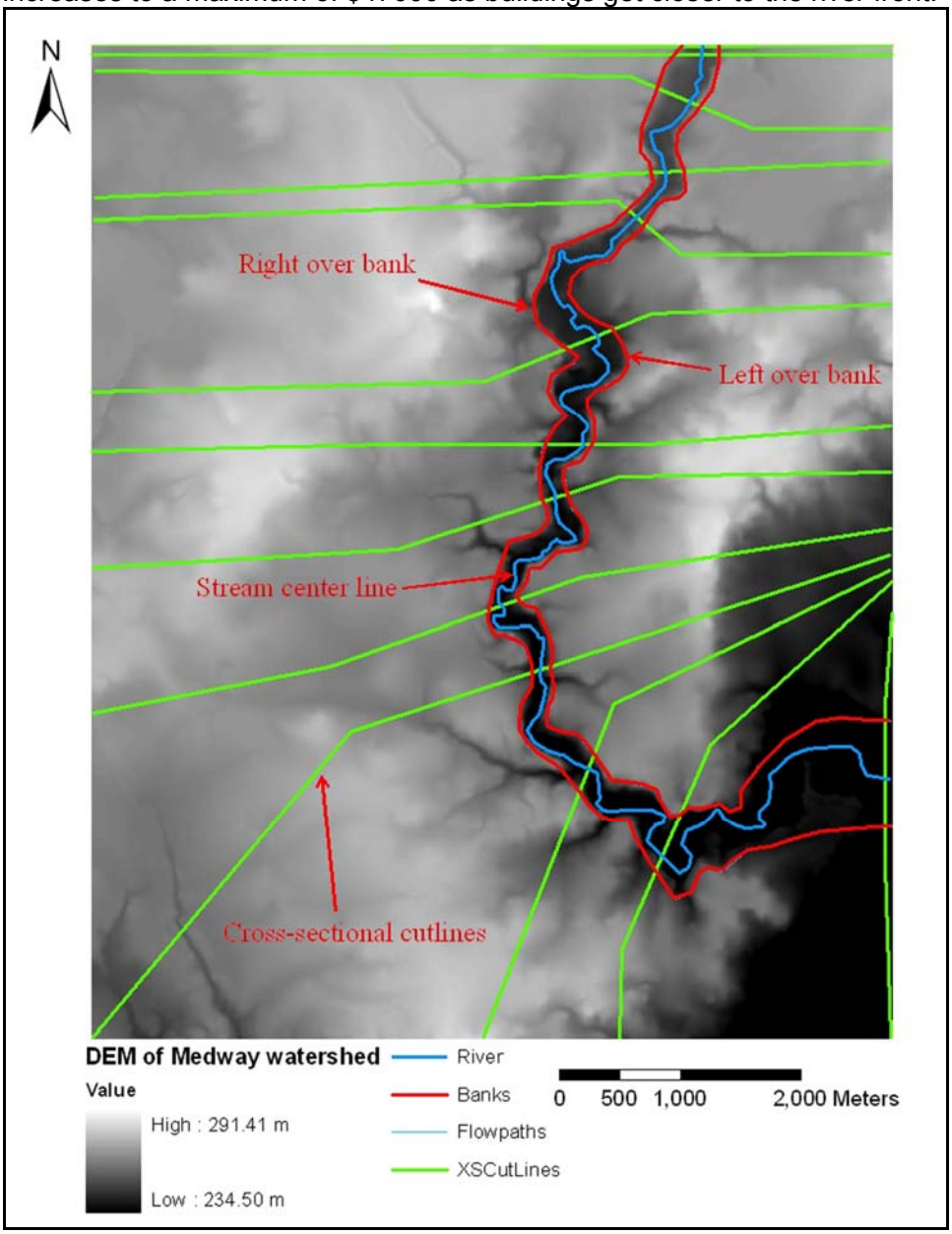


Figure 18 GIS data

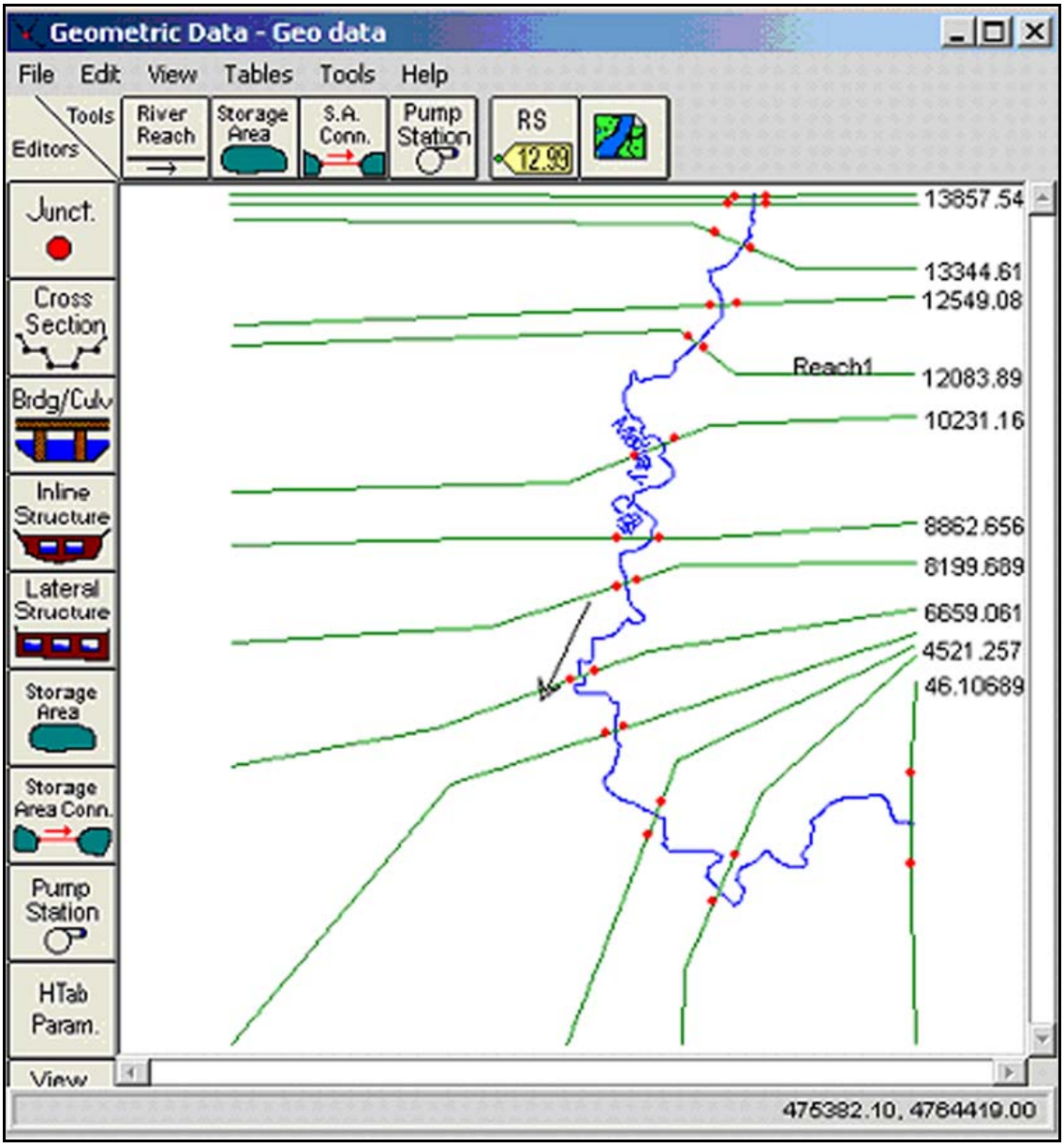


Figure 19 RAS GIS themes imported from HEC-GeoRAS to HEC-RAS

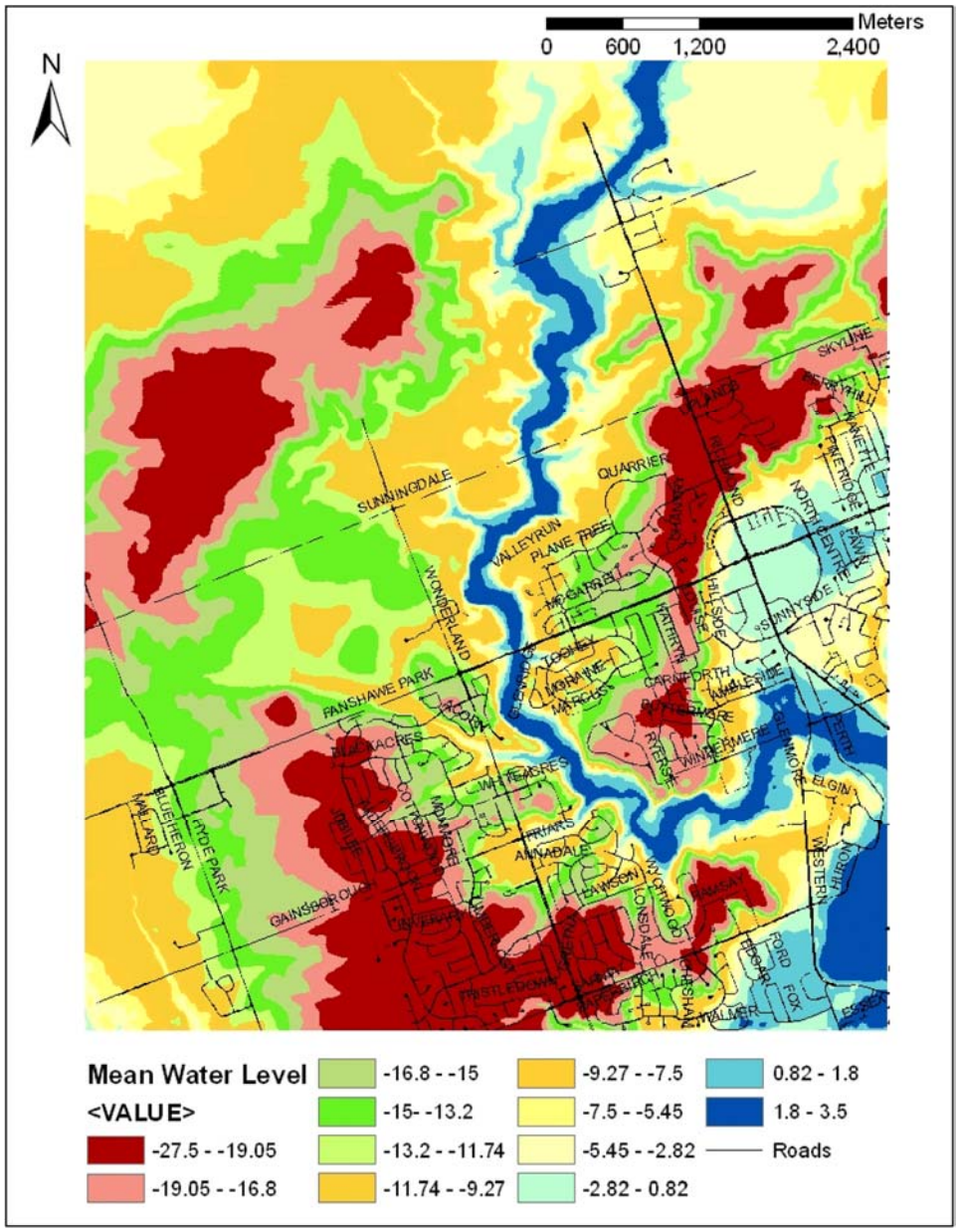


Figure 20 Difference in water surface elevation and ground surface elevation (in meters) for the modal value of water level

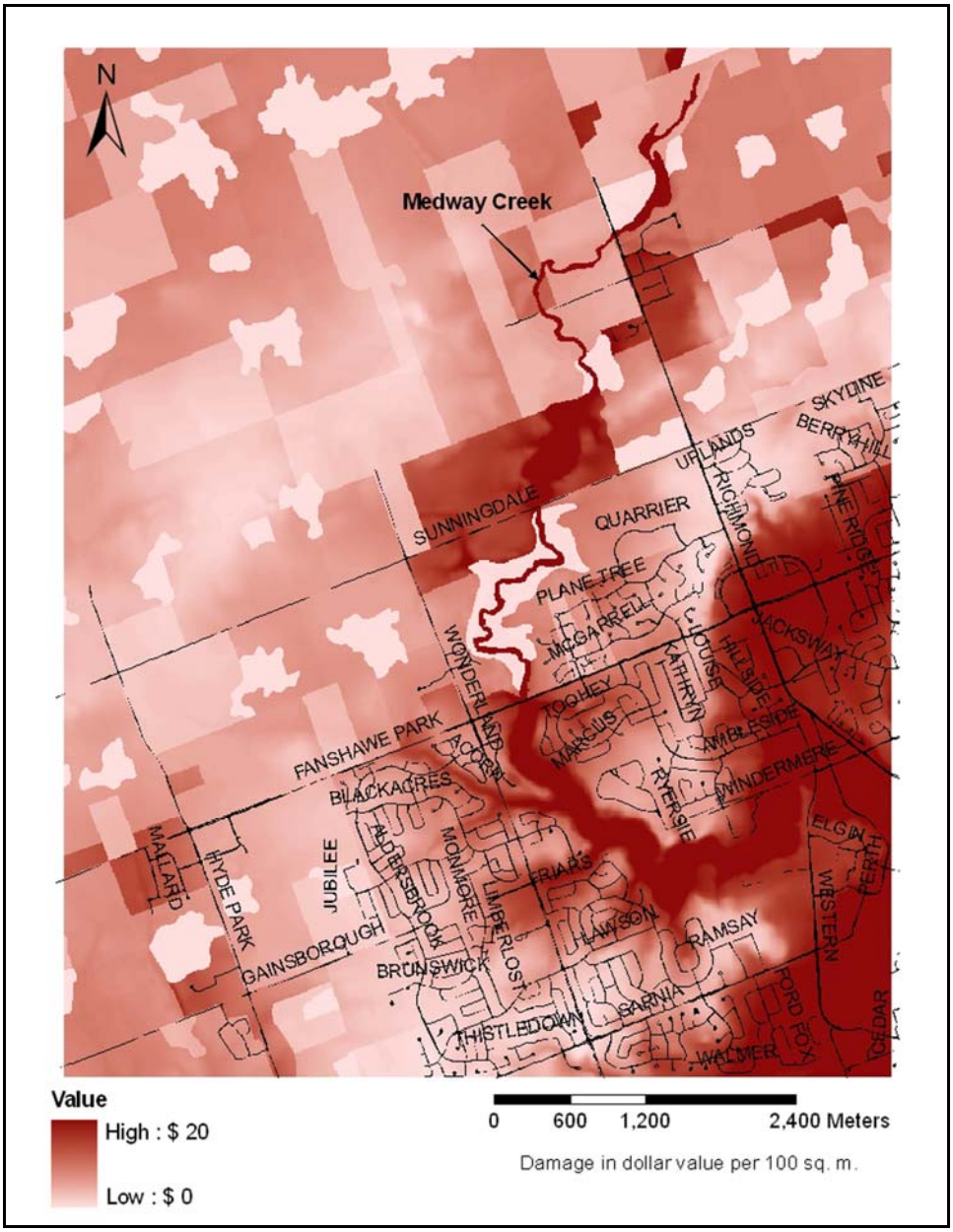


Figure 21 Land damage based on the modal value of water level

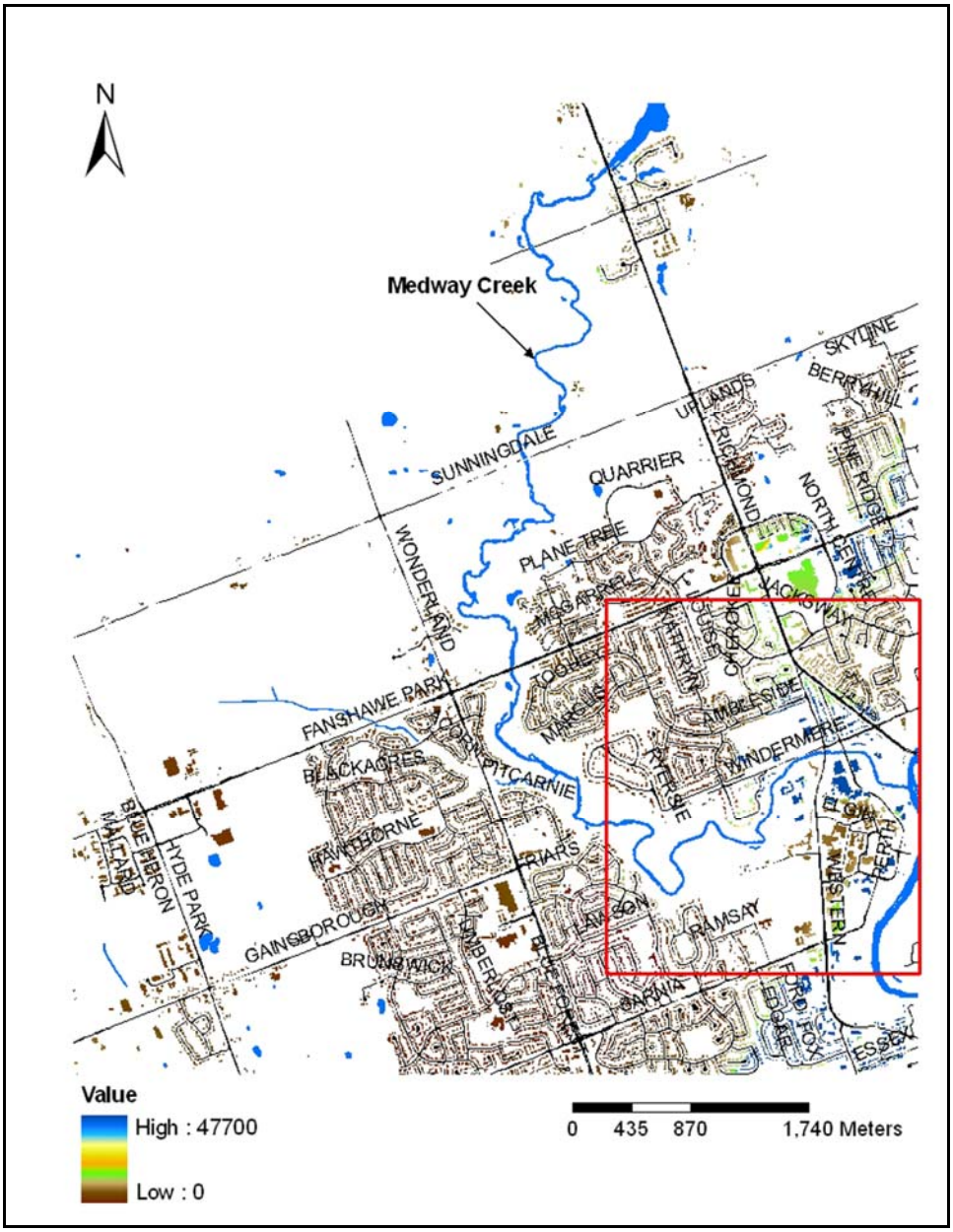


Figure 22 Damage to one and two story buildings with basement based on the modal value of water level

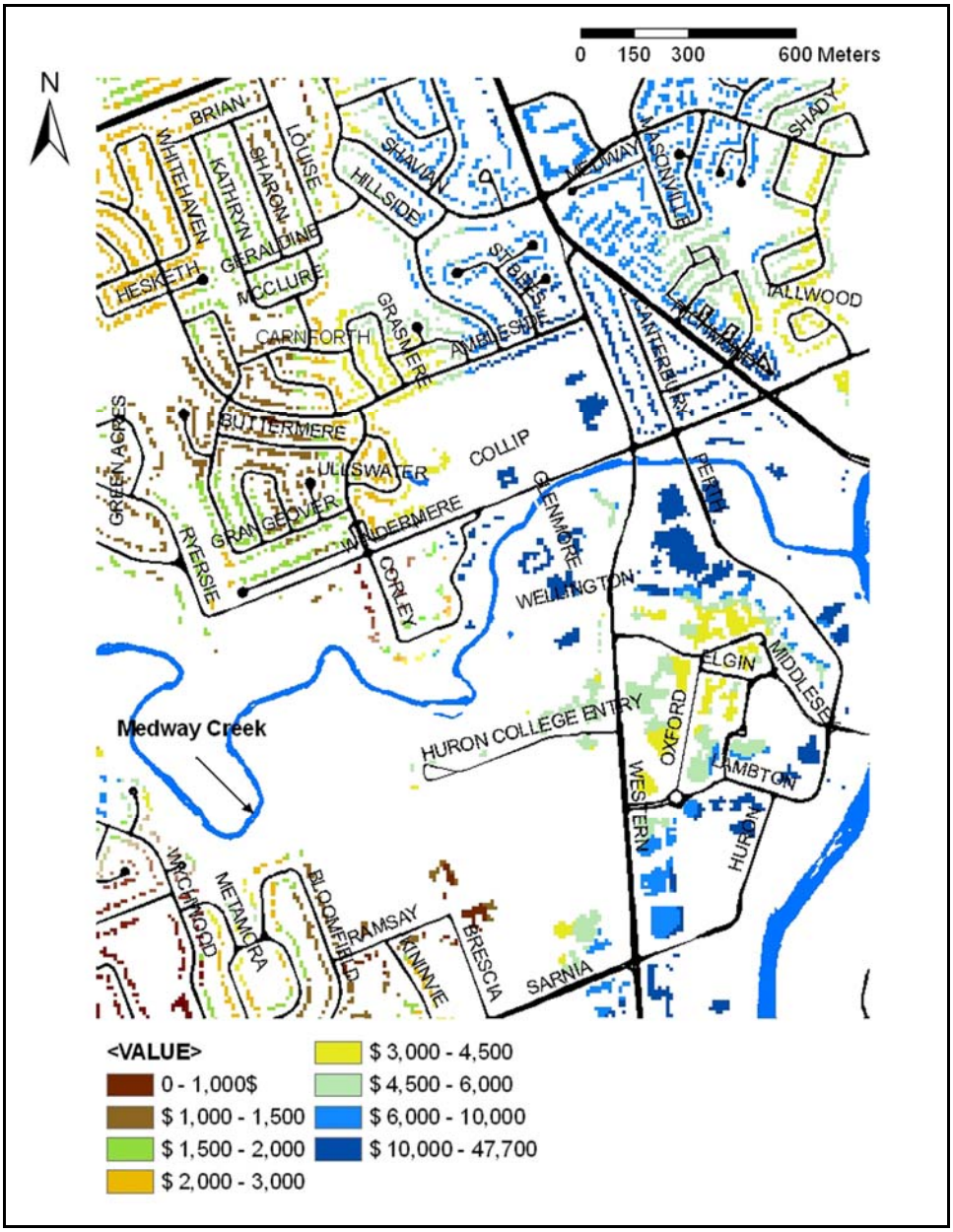


Figure 23 Reclassification of damage to one and two story buildings with basement based on the modal value of water level

3.3 Spatial Combined Fuzzy Reliability-Vulnerability of the Medway Creek

The quantitative analysis of maps of the entire study region containing compatibility values for conservative, neutral and risky level of flood damage are provided in Table 1. Change from one acceptable level to another results in change of the overlapping area that is used to measure compatibility. About 12.22 km^2 of the Medway Creek region belongs to low compatibility value (zero) for the conservative level of the acceptable flood damage (Table 1). In the case of neutral acceptable level of the flood damage, area of 9.97 km^2 shows zero compatibility. In the case of risky acceptable level of the flood damage, area of 3.32 km^2 shows zero compatibility. At higher level of compatibility (for example value of one) areas of the Medway Creek corresponding to

conservative, neutral and risky levels of the acceptable flood damage are 8.91 km^2, 14.07 km^2 and 23.42 km^2, respectively. As expected, an increase in the acceptable level of flood damage results in larger area of the study region with higher compatibility value.

Compatibility value	Area (Km^2) corresponding to different level of the acceptable flood damage			Percent change in area for changing levels of the acceptable flood damage		
	Conser-vative level of damage	Neutral level of damage	Risky level of damage	from conser-vative to neutral	from neutral to risky	from conser-vative to risky
0.00	12.22	9.97	3.32	-18.00	-67.00	-73.00
0.10	6.57	1.71	2.65	-74.00	55.00	-60.00
0.20	4.51	1.34	1.53	-70.00	14.00	-66.00
0.30	3.88	4.95	1.54	28.00	-69.00	-60.00
0.40	2.90	3.81	1.05	32.00	-72.00	-64.00
0.50	2.77	4.14	1.12	50.00	-73.00	-60.00
0.60	3.28	3.12	1.24	-5.00	-60.00	-62.00
0.70	2.92	3.16	5.06	8.00	60.00	73.00
0.80	2.55	4.07	6.75	59.00	66.00	165.00
0.90	3.81	3.97	6.63	4.00	67.00	74.00
1.00	8.91	14.07	23.42	58.00	66.00	163.00

Table 1 Area and percent change in the area of the study region corresponding to different compatibility value and different level of the acceptable flood damage

The increase in acceptable level of the flood damage results in the decrease of lower percentage of the Medway Creek area having low compatibility, and the increase in high percentage of the Medway Creek area having high compatibility. For example, at 0.9 compatibility value (Table 1) increase in area is about 4% for the switch from conservative to neutral level of the acceptable flood damage, and 74% for the switch from conservative to risky level of the acceptable flood damage.

Quantitative analysis of compatibility is also performed for different land use within the City of London. Following land use categories are considered: hay land; land with continuous row crop; and grain land. Amount of land under various land use categories is given for three different acceptable levels of the flood damage for different compatibility values in Figures 24, 25 and 26. Results show that land having lower level of damage shows higher value of compatibility. For

the conservative level of the acceptable flood damage, hay land having lowest damage shows the maximum compatibility value (Figure 24). Compatibility of the agricultural land containing row crop and corn shows higher damage in comparison to the land with hay. As the acceptable level of flood damage increases to neutral (Figure 25) and risky (Figure 26), the compatibility value increases too.

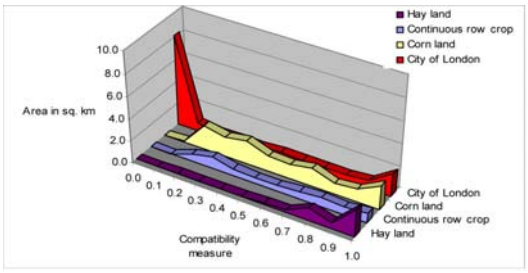


Figure 24 Land use compatibility for the first (conservative) acceptable level of damage

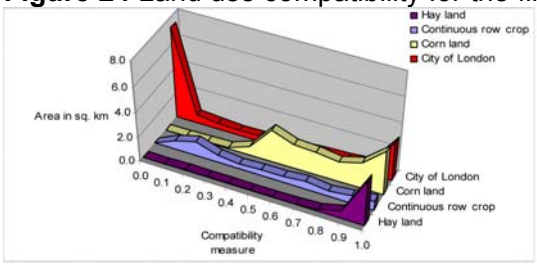


Figure 25 Land use compatibility for the second (neutral) acceptable level of damage

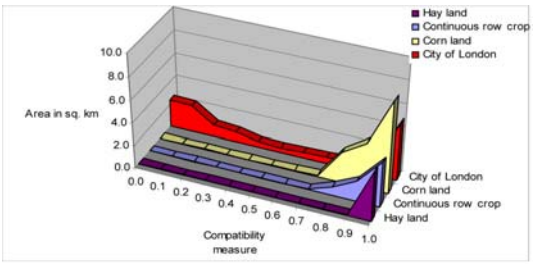


Figure 26 Land use compatibility for the third (risky) acceptable level of damage

Quantitative analyses of the maps for different compatibility values show that the largest area with maximum compatibility is achieved for the risky acceptable level of the flood damage. Therefore the compatibility value map for the risky level of acceptable flood damage is used in the development of the of spatial combined fuzzy flood reliability-vulnerability index map of the Medway Creek in Figure 27. The combined fuzzy flood reliability-vulnerability index is shown in Figure 27 in the range from zero to one. The maximum value that the combined fuzzy reliability-vulnerability index can attain is one. If the actual system has a combined fuzzy reliability-vulnerability index of one then the system is considered safe or highly reliable with low vulnerability. If the value of combined fuzzy reliability-vulnerability index is zero, then the system is considered unsafe with low reliability and high vulnerability. In this study a color ramp is used (Figure 27) to show the combined fuzzy flood reliability-vulnerability index of the Medway Creek. Blue color is used to show low value of the combined fuzzy flood reliability-vulnerability index and the high value is shown in dark brown color.

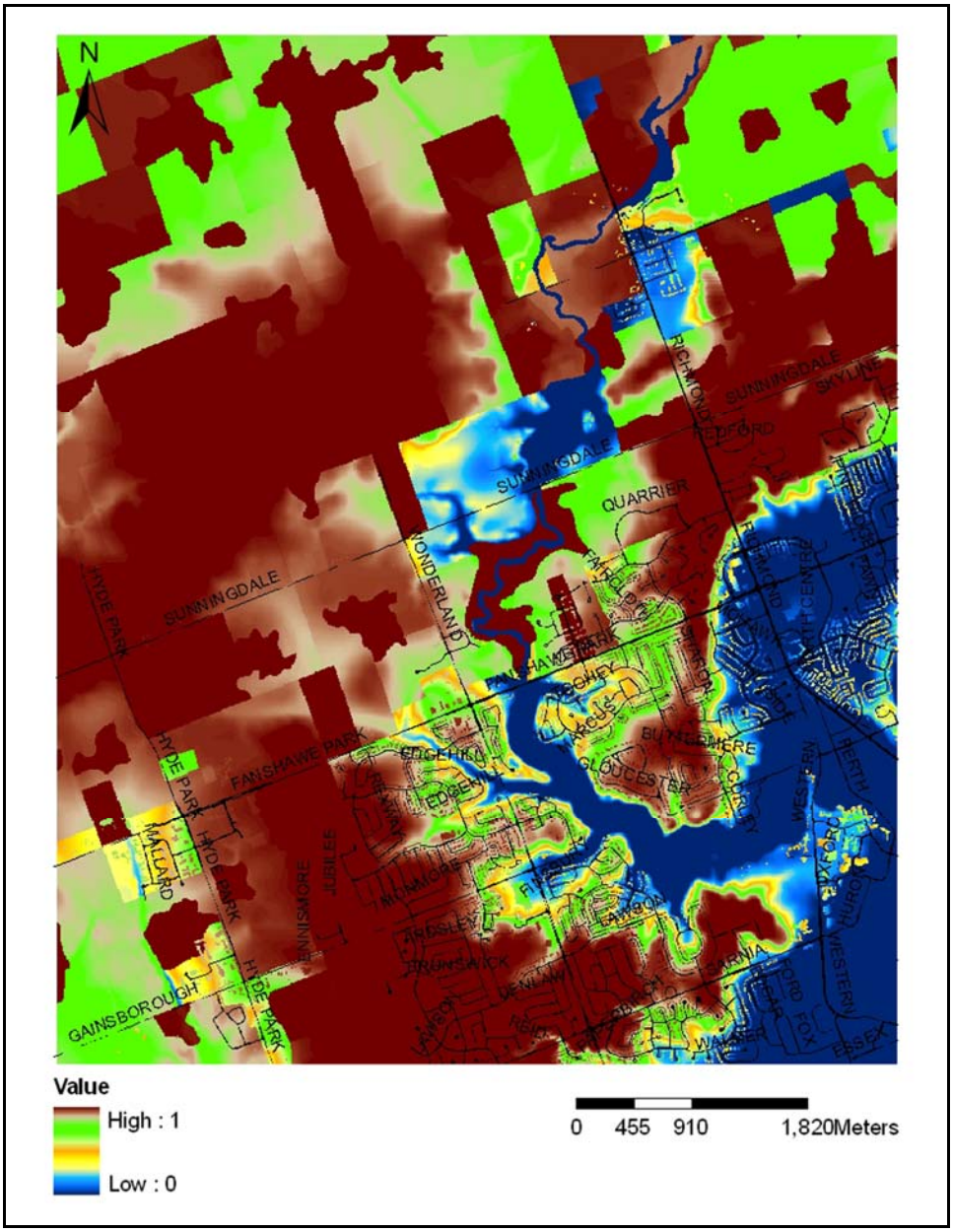


Figure 27 The fuzzy flood reliability-vulnerability index for the Medway Creek

The combined fuzzy flood reliability-vulnerability index for a region or a location of particular interest can be easily identified using the color ramp. Land close to the Medway Creek is found to have low level of flood reliability and high vulnerability. The combined fuzzy flood reliability-vulnerability index value ranges from 0 (dark blue) to 0.3 (light blue). Yellow marks the areas of higher reliability and lower vulnerability compared to the regions closer to the river. Value of the combined fuzzy flood reliability-vulnerability index in this region is between 0.31 (light yellow) and 0.45 (dark yellow). Transition to regions with high reliability is indicated by the value of combined index in the range of 0.46 (dark orange) to 0.6 (light orange). Green marks the regions that are more reliable and less vulnerable to floods and the index value is between 0.61 and 0.89. Regions with highest reliability are shown in brown color with the index value between

0.9 (light brown) and 1.0 (dark brown). The region close to the confluence of the Medway Creek and the North Thames is the most prone to flooding. Areas such as these show a very low value of the combined fuzzy reliability-vulnerability index of 0 to 0.3.

Comparison of the Medway Creek DEM with the map in Figure 27 shows, as expected, that the regions of low ground surface elevation are at higher risk from flooding and therefore have a very low combined fuzzy reliability-vulnerability index. The residential area near the confluence may suffer significant flood damage and large area in the south-east part of the map shows low reliability and high vulnerability. Amount of land under various land use categories is given for different combined fuzzy reliability-vulnerability values in Figures 28. Approximately 6.77 km^2 of the southern part of the study region near the river (43% of the City of London on the map) is the area of very low reliability (index value from 0 to 0.3). Western part of the study region, 6.14 km^2 (39% of the City of London on the map) is the area of high reliability (index value from 0.9 to 1).

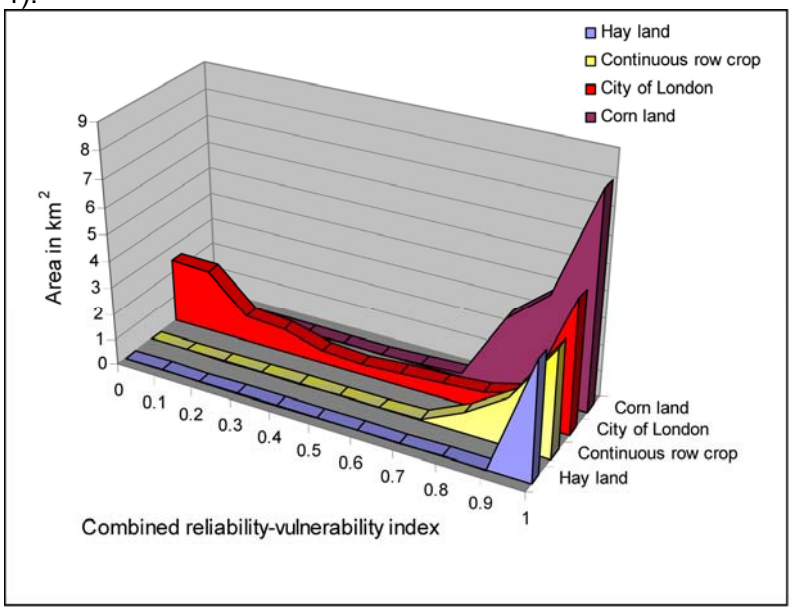


Figure 28 Combined reliability–vulnerability index for different landuse

Areas north of the City (northern part of the study region) are mainly agricultural. It is found that the combined fuzzy flood reliability-vulnerability increases in the northern direction. This is contributed to the fact that the flood damage to agricultural land is lower than the flood damage to residential land. Almost 98% of the agricultural land under continuous row crop and corn shows the index value between 0.7 and 1.0. Almost 99% of the land under hay has the index value between 0.9 and 1.0. The change in the combined fuzzy flood reliability-vulnerability index is clearly seen on the map - many regions within the urban part of the City of London are in blue (low reliability and high vulnerability); north of the City, the agricultural regions show a transition from blue to green and brown (higher reliability and lower vulnerability).

3.4 Spatial Fuzzy Robustness of Medway Creek

The fuzzy robustness index is directly related to the change in fuzzy compatibility value. The higher the change in compatibility value, the lower the value of fuzzy robustness index and vice-versa. The higher the value of the fuzzy robustness index, the higher the systems ability to adapt to changing conditions. Fuzzy flood robustness index of the Medway Creek is expressed

using a color ramp, with blue representing location with low robustness and dark brown with high robustness (Figures 29, 30 and 31).

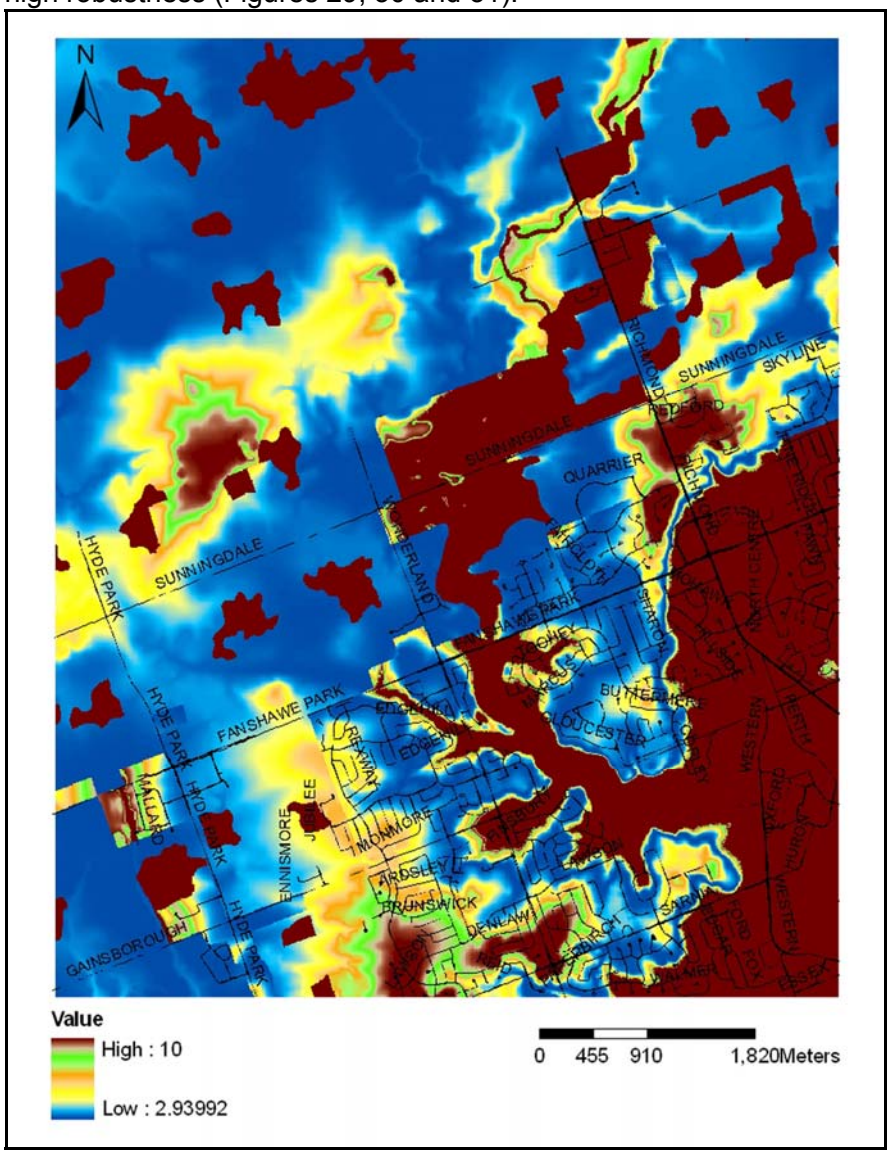


Figure 29 Fuzzy flood robustness index of the Medway Creek for the change from conservative to neutral acceptable level of flood damage

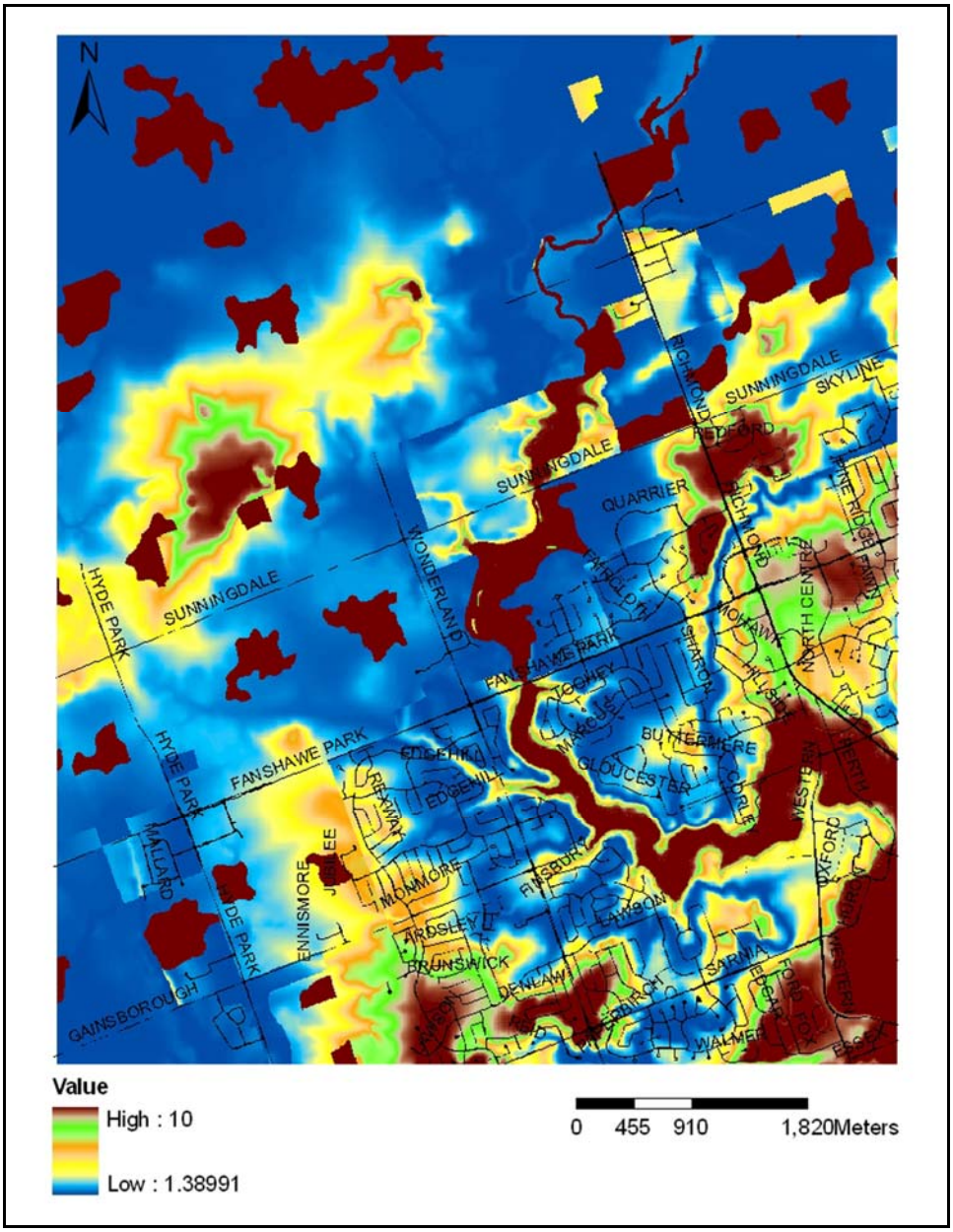


Figure 30 Fuzzy flood robustness index of the Medway Creek for the change from conservative to risky acceptable level of flood damage

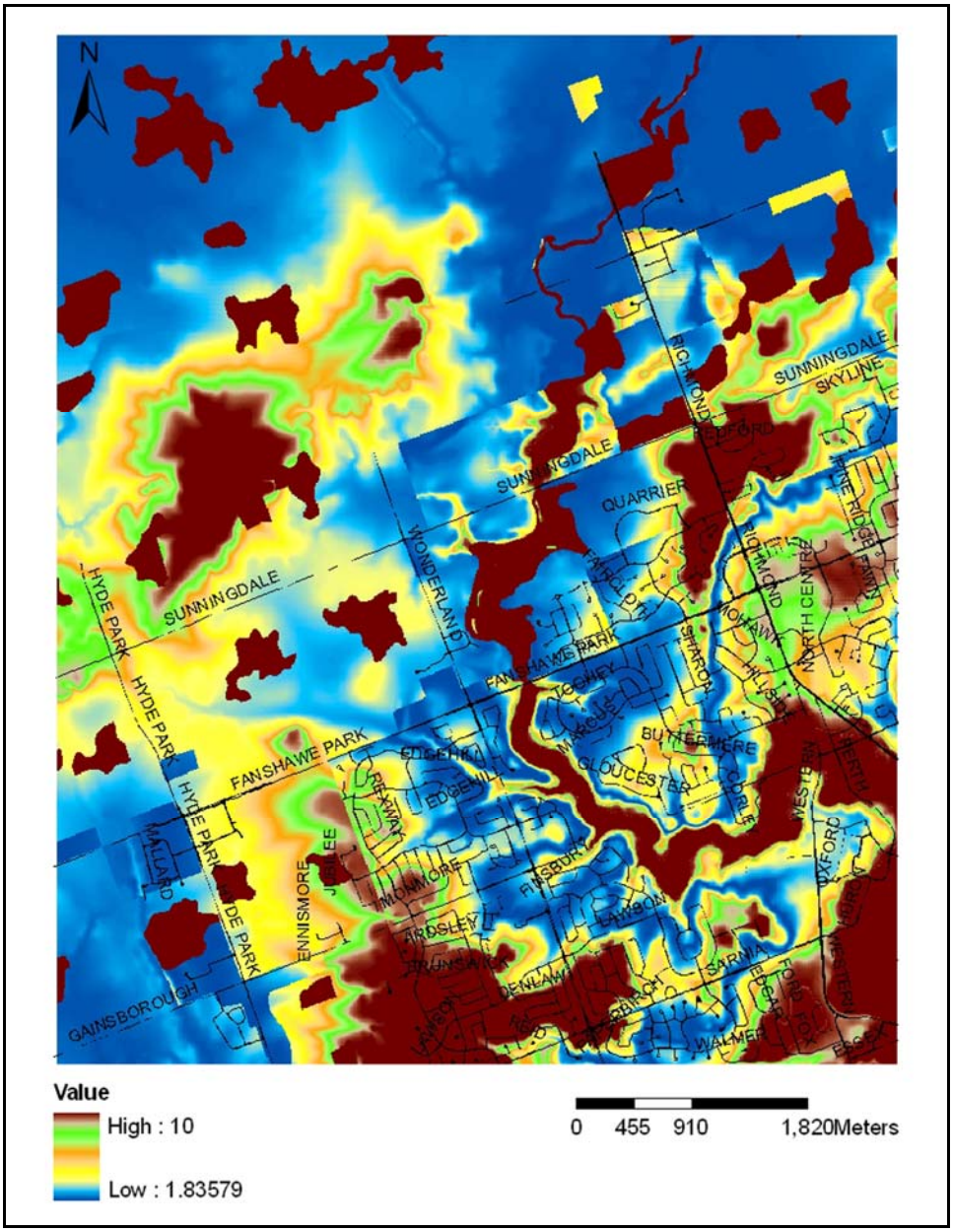


Figure 31 Fuzzy flood robustness index of the Medway Creek for the change from neutral to risky acceptable level of flood damage

When the acceptable level of flood damage changes from a conservative level to a neutral level, the fuzzy flood robustness index value is in the range from 2.94 (less robust) to 10 (highly robust). Areas near the river and the confluence on the map in Figure 29 are shown in blue (fuzzy flood robustness index value between 2.94 and 4.25). Land close to the Medway Creek and the confluence shows lower robustness compared to the areas further away from the river which are shown in yellow (index range from 4.25 to 6.3), orange (index range from 6.3 to 7.10), green (index range from 7.11 to 9.3) or brown (index range from 9.4 to 10).

Adaptation to change in the acceptable level of flood damage from conservative to risky is more difficult and the value of fuzzy flood robustness index decreases. Map in Figure 30 shows areas near the river and the confluence with much lower value of the fuzzy flood robustness index, from 1.39 to 3.

When the acceptable level of flood damage changes from neutral to risky (Figure 31), the fuzzy flood robustness index shows lower decline compared to the change from conservative to risky level of the acceptable flood damage. Amount of land for different values of robustness for changing the acceptable levels of damage is shown in Figures 32. In the case of change from conservative to neutral level, approximately 7.97 km^2 of the study region shows robustness index between 1 and 3. For change from neutral to risky and conservative to risky, the area increases to 23.3 km^2 and 32.4 km^2, respectively. The more drastic change in the acceptable level of flood damage results in lower robustness. Also, locations further away from the river and low lying areas show higher robustness to flooding.

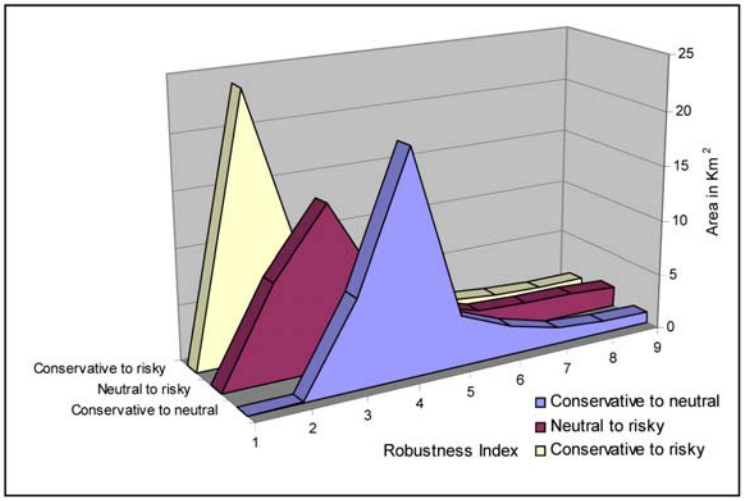


Figure 32 Area corresponding to robustness index for changing the acceptable level of damage

3.5 Spatial Fuzzy Resiliency of Medway Creek

Fuzzy resiliency index of the Medway Creek is shown using a colour ramp in Figure 33. The dark blue color represents lowest resiliency value i.e 0; therefore low ability for a quick recovery. Dark brown colour represents the highest resiliency, i.e 1.97; therefore high ability of the area for a quick recovery. It is found that areas closer to the Medway Creek and also the region close to the confluence of the Medway Creek and the North Thames experience decrease (shown in blue) in the fuzzy resiliency index. The resiliency index for these region ranges from 0 (dark blue) to 0.23 (light blue). Due to low lying areas just north and south of the confluence, submerged areas need more time to recover and therefore result in low resiliency. Near the confluence the residential area requires more flood damage recovery time and therefore large area in the south-east part of the map shows low resiliency that ranges from 0 to 0.23. Regions outside the floodplain show higher resiliency as they are shown in map in yellow (ranges from 0.24 to .34), orange (ranges from 0.35 to 0.45), green (ranges from 0.46 to 0.6) and brown (ranges from .61 to 1.97). North of the City of London, agricultural land shows higher resiliency (marked in green and brown) compared to residential lands. The map showing values of fuzzy resiliency index is a very useful indication of the region's ability for a quick recovery that may be used in planning flood emergency and recovery effort.

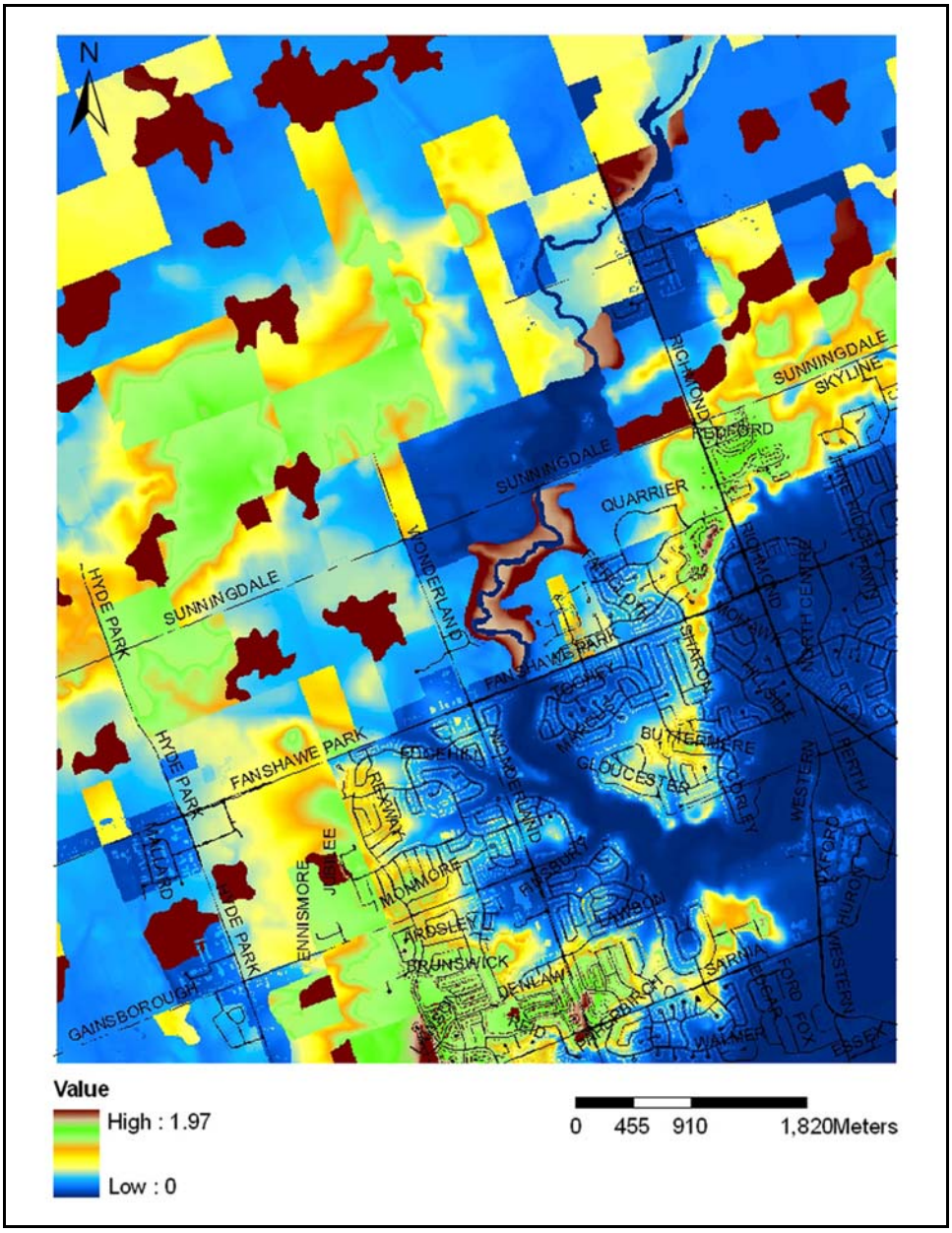


Figure 33 Fuzzy flood resiliency index of the Medway Creek

4. Conclusions

This paper presents a new approach for addressing spatial variability of uncertainty in water resources management. Developed methodology can address spatially variable risk from natural hazards such as floods, cyclones, storm surges and even environmental pollution. Fuzzy reliability indices are extended in space to account for spatial variability in natural hazard risk assessment and management. A detailed methodology is presented for spatial assessment of risk through the calculation of reliability, vulnerability and resiliency of a system under threat. Spatial combined fuzzy reliability-vulnerability index is used to assess the frequency and severity of disaster threat. This map can be used to identify areas of potential hazards and is

useful in risk mitigation process and can also aid the decision making during emergency. Spatial fuzzy robustness index is used to assess the ability of the area to adapt to a wide range of possible hazard conditions. The time required for an area to recover from disaster has been assessed using a spatial fuzzy resiliency index. The GIS is used to capture the spatially distributed information for fuzzy reliability analysis.

Fuzzy reliability indices implemented through the GIS are used to illustrate the proposed methodology for the flood reliability analysis of the Medway Creek within the City of London. A floodplain map is generated first for the study region and then the damage is estimated based on the depth-damage relationships. This work examines the damage that may occur to buildings, residential and agricultural lands based on the 500 year flood. Fuzzy reliability indices are used to assess the ability of the study area to withstand possible flooding conditions.

Ambiguity in the definition of failure is expressed by the fuzzy membership function of acceptable level of flood damage. As the acceptable level of flood damage increases, more land becomes exposed to the higher level of flood damage. Different patterns of spatial compatibility are obtained from the various land use categories. Areas prone to higher flood damage are less compatible compared to the areas that are less prone to flood damage. Increasing the acceptable level of flood damage results in higher compatibility for all land use categories.

The final results of the fuzzy flood reliability analysis are presented using maps that show the variation of reliability-vulnerability, robustness and resiliency in space. Quantitative analysis of maps generated by the proposed methodology shows that the high acceptable level of flood damage can result in larger area of high flood reliability and high flood resiliency and the low acceptable level of flood damage can result in low flood reliability and low flood resiliency. Implementation of the fuzzy reliability indices in space provides additional information on flooding risk that may be of value to water authorities, general public and insurance industry. Thus, GIS based risk modeling of spatial fuzzy reliability indices is an effective and efficient approach to capture the spatial variation of risk related to natural hazards and can assist in the minimization of damage.

Acknowledgment
Funding from the Public Safety and Emergency Preparedness (PSEP) and the National Sciences and Engineering Research Council (NSERC) of Canada to carry out this work is greatly appreciated.

References
Ahmad, S. S.; Simonovic, S. P. 2006. ‘A New Method for Spatial Fuzzy Reliability Analysis of Floods’. *Water Resour. Res,* Under review.
Ang, H-S.; Tang, H.1984. *Probability Concepts in Engineering Planning and Design*. New York, USA: John Wiley & Sons, Inc.
Akter, T.; Simonovic, S. P. 2005. ‘Aggregation of fuzzy views of a large number of stakeholders for multi-objective flood management decision-making’. *Journal of Environmental Management* 77, (2): 133-134.
Bender M. J.; Simonovic, S. P. 2000. ‘A Fuzzy Compromise Approach to Water Resources Systems Planning Under Uncertainty’. *Fuzzy Sets and Systems* 115: 35-44.
Borsuk, M.; Clemen, R.; Maguire, L.; Reckhow, R. 2001. ‘Stakeholder Values and Scientific Modeling in the Neuse River Watershed’. *Group Decision and Negotiation* 10: 355–373.

Coppock, J.T. 1995. 'GIS and natural hazards: an overview from a GIS perspective'. In Carrara, A., Guzzetti, F. (eds.) *Geographical Information Systems in Assessing Natural Hazards*. Vol. 6. Kluwer Academic, Netherlands, 21-34.
Despic, O.; Simonovic, S. P. 2000. 'Aggregation operators for soft decision making'. *Fuzzy Sets Systems* 115 (1): 11–33.
El-Baroudy, I.; Simonovic, S. P. 2004. 'Fuzzy criteria for the evaluation of water resource systems performance' *Water Resour. Res.* 40, W10503, doi: 10.1029/2003WR002828.
El-Baroudy, I.; Simonovic, S. P. 2006. 'A Decision Support System for Integrated Risk Management'. Technical report. University of Western Ontario, Facility for Intelligent Decision Support, London, Ontario, Canada.
Emmi, P. C.; Horton, C. A. 1995. 'A Monte Carlo simulation of error propagation in a GIS-based assessment of seismic risk' *International Journal of Geographical Information Systems* 9: 447-461.
Foster, J. A.; McDoDonald, A. T. 2000. 'Assessing pollution risks to water supply intakes using geographical information systems (GIS)'. *Environmental Modelling and Software* 15: 225-234.
Ganoulis, J.G. 1994. *Engineering Risk Analysis of Water Pollution: Probabilities.* Netherlands, Weinheim: VCH.
Hashimoto, T.; Stedinger, J. R.; Loucks, D. P. 1982a. 'Reliability, Resiliency, and Vulnerability Criteria for Water Resources System Performance Evaluation'. *Water Resour. Res.* 18 (1): 14-20.
Hashimoto, T.; Loucks, D. P.; Stedinger, J. R. 1982b. 'Robustness of Water Resources Systems'. *Water Resour. Res.* 18 (1): 21-26.
Hydraulogic Engineering Center. 2005. *HEC-GeoRAS GIS Tools for support of HEC-RAS using ArcGIS, Users Manual, Version 4.* United States Army Corps of Engineers.
Kacprzyk, J.; Nurmi, H. 1998. 'Group Decision Making Under Fuzziness'. In Slowinsky, R. (eds.) *Fuzzy Sets in Decision Analysis*. Operation Research and Statistics, Kluwar Academic Publishers.
Kwok, R.C.W., Ma, J.; Zhou, D. 2002. 'Improving Group Decision Making: A Fuzzy GSS Approach'. *IEEE Transactions on Systems, Man, and Cybernetics-Part C: Applications and Reviews* 32 (1): 54-63.
Makropoulos, C.K.; Butler, D. 2004. 'Spatial ordered weighted averaging: incorporating spatially variable attitude towards risk in spatial multi-criterial decision making'. *Environmental Modelling and Software* 21: 69-84.
Makropoulos, C.K.; Butler, D.; Maksimovic, C. 2003. 'Fuzzy Logic Spatial Decision Support System for Urban Water Management'. *Journal of Water Resources Planning and Management* 129 (1): 69-77.
Modarres, M.; Kaminsky, M.; Kriotsov, V. 1999. *Reliability Engineering and Risk Analysis: A Practical Guide,* New York: Marcel Dekker.
Ontario Ministry of Natural Resources (Minister- Lyn McLeod). 1990. *Flood Damage Estimation Guide.* Queen's Printer for Ontario.
Prodanovic, P.; Simonovic, S.P. 2002. 'Comparison of fuzzy set ranking methods for implementation in water resources decision-making'. *Canadian Journal of Civil Engineering* 29: 692-701.
Press, S. J. 2003. *Subjective and Objective Bayesian Statistics: Principles, Models, and Applications.* Hoboken, N. J: John Wiley.
Rejeski, D. 1993. 'GIS and risk: a three culture problem'. In Goodchild, M. F.; Parks, B. O.; Steyaert, L. T. (eds.) *Environmental Modeling with GIS.* Oxford University Press, New York, 318-331.
Simonovic, S. P. 1997. 'Risk in sustainable Water Resources Management'. In *proceedings of Sustainability of Water Resources Under Increasing Uncertainty: the Rabat Symposium, IAHS Publ.,* 240: 3-17.

Simonovic, S. P.; Nirupama 2005. 'A spatial multi-objective decision making under uncertainty for water resources management'. *Journal of Hydroinformatics* 7 (2): 117-133.
Upper Thames River Conservation Authority (UTRCA) 2001. 'Medway Creek Watershed Report Card'. Accessed 6 September 2006. Available from: http://www.thamesriver.on.ca/Watershed_Report_Cards/images/MedwayCreek.pdf
Vick, S.G. 2002. *Degrees of Belief: Subjective Probability and Engineering Judgment*. USA: ASCE Press.
Zadeh, L. A. 1965. 'Fuzzy Sets' *Information and Control* 8: 338-353.
Zerger, A. 2002. 'Examining GIS decision utility for natural hazard risk modeling'. *Environmental Modelling and Software* 17: 287-294.
Zimmermann, H.-J. 1996. *Fuzzy Set Theory and its Applications.* 3rd Edition. Massachusetts, USA: Kluwer Academic Publishers.